Chapter 17

Iterative Solutions for Mobility Problems

The solution of large linear systems is best accomplished by some iterative method. Such methods are available if an approximate inverse for the coefficient matrix can be (inexpensively) constructed, or if the matrix satisfies certain conditions so that direct iteration is possible.

The spectrum of the double layer integral operator will be inspected, and we shall show how the operator can be modified so that this modified analytic operator satisfies the conditions for feasibility of direct iteration. If the discretized linear system closely enough approximates the analytical equations, we may expect it to share the same properties, thus allowing direct iterative solution.

17.1 Conditions for Successful Direct Iteration

Here we shall briefly discuss the direct, or Picard, iteration. Let $\mathcal{K}$ be a linear operator on a Hilbert space and b a given vector. On trying to solve the equation $x = \mathcal{K}x + b$ for x, it seems natural to try the iteration $x_{i+1} = \mathcal{K}x_i + b$ — note that the second kind IEs are directly of this form. Suppose the iterations are started with the approximate solution x_1, and consider the errors $z_i = x_i - x$. These errors satisfy the recursion relation $z_{i+1} = \mathcal{K}z_i$ from which by induction $z_i = \mathcal{K}^{i-1}z_1$. For the errors to vanish in the limit of a large number of iterations, regardless of how the initial guess x_1 was chosen, it is necessary and sufficient that the powers of $\mathcal{K}$ vanish in the limit of large exponents. For compact operators $\mathcal{K}$ this condition is equivalent to requiring the *spectral radius* of $\mathcal{K}$ to be strictly less than one. The spectral radius is by definition the largest, of all absolute values of the eigenvalues of $\mathcal{K}$. Finite matrices are compact operators, so that in particular the result mentioned applies to ordinary matrices as well.

Assume for the moment that $\mathcal{K}$ would have an eigenvalue larger or equal to one in absolute magnitude. Then it is easy to see that the iterations will not converge if the initial error vector z_1 is the corresponding eigenvector, as

on each iteration this is just multiplied with the eigenvalue. This shows the necessity of the condition on the spectral radius.

Assume now that all the eigenvalues of $\mathcal{K}$ are less than one in absolute magnitude. If z_1 is an eigenvector, clearly the error will go to zero in the limit. Suppose z_1 is a principal vector such that $(\lambda 1 - \mathcal{K})z_1$ is an eigenvector z. Then $\mathcal{K}z_1 = \lambda z_1 - z$ and by induction $\mathcal{K}^i z_1 = \lambda^i z_1 - i\lambda^{i-1}z$, which again tends to zero since $|\lambda| < 1$. This argument can be extended to principal vectors further back in the Jordan chain with induction. Finally, as any initial guess vector z_1 can be represented in the basis formed by the eigenvectors and other principal vectors, it is sufficient to inspect these separately, as was done above. This shows (readers desiring complete rigor are referred to textbooks on mathematics) the sufficiency of the condition on the spectral radius. Also please note how the errors in the directions of the proper vectors decrease with iterations as the powers of the corresponding eigenvalue — the spectral radius gives the dominating eigenvalue, and therefore characterizes the rate of convergence. In our case the double layer operator in fact is diagonalizable (see the exercises), so that discussion of other principal vectors than eigenvectors is just for the sake of generality.

The direct iteration scheme is naturally not the only possible one, but it is the simplest and suffices for the application to be presented. Sometimes an *approximate inverse* H is known for the system matrix $1 - K$, such that $H(1 - K)$ is very nearly identity. Then the original equation can be written as $x = [1 - H(1 - K)]x + Hb$, by a small rearrangement after premultiplication with H, and now the bracketed "iteration operator" here is small enough (in terms of the spectral radius) to allow direct iteration. As a final note we observe that any operator norm derived from a vector norm by $|\mathcal{K}| = \sup |\mathcal{K}x|/|x|$ gives an upper bound for the spectral radius and thus can be used to show the feasibility of iterative solutions.

17.2 The Spectrum of the Double Layer Operator

In this section two results given by Odqvist [53] for single bounding surfaces shall be established in the multiboundary setting, namely, that the spectra of the operators $\mathcal{K}$ and $\mathcal{K}^*$ are real and therefore coincide, and this common spectrum is within the interval $[-1, 1]$. Since Odqvist omits the details, our exposition more closely follows that given in Karrila [37]. As the reader may recall, in general the spectra of an operator and its adjoint are mapped to each other by complex conjugation (see Section 14.2.5). The eigenvalues of $\mathcal{K}$ at the endpoints of this interval were already examined in the theorems within this chapter, since these are the physically relevant ones.

In the following complex conjugation shall be denoted by the superscript c.

For complex surface fields in L_2 the natural inner product is

$$\langle \boldsymbol{f}, \boldsymbol{g} \rangle = \oint_S \boldsymbol{f} \cdot \boldsymbol{g}^c \, dS \ . \tag{17.1}$$

A complex Stokes solution is such that its real and imaginary parts are ordinary Stokes solutions. The stress field is defined as before and will also be complex. By using the Lorentz reciprocal theorem for real homogeneous Stokes solutions, and the linearity of the operation of taking the stresses, one can verify that the Lorentz reciprocal theorem is valid for complex Stokes fields in the form:

$$\langle \boldsymbol{v}, \hat{\boldsymbol{n}} \cdot \boldsymbol{\sigma}(; \boldsymbol{u}) \rangle = \langle \hat{\boldsymbol{n}} \cdot \boldsymbol{\sigma}(; \boldsymbol{v}), \boldsymbol{u} \rangle \ . \tag{17.2}$$

Also the dissipation of a complex velocity field is the sum of the dissipations of its real and imaginary parts, and is given by $\langle \boldsymbol{v}, \hat{\boldsymbol{n}} \cdot \boldsymbol{\sigma}(; \boldsymbol{v}) \rangle$. Thus the dissipation is always non-negative and is zero only if there is complex RBM.

Let ψ be a complex single layer eigenfunction on the totality of bounding surfaces S. *If the total dissipation* (sum of dissipations in the interior and the exterior) *is zero*, then there can be only RBM in each connected component of the interior and exterior. Thus on each of these there is a constant pressure, and the single layer density being proportional to the traction jumps over surfaces is a multiple of the surface normal on each surface. A constant multiple of the surface normal $p\hat{\boldsymbol{n}}$ on a container surface will give zero stress on the outside, $-p\hat{\boldsymbol{n}}$ on S_c (Theorem 2), and the constant pressure field $-2p\boldsymbol{\delta}$ as the stress field on the inside. On a particle surface the main difference is the direction of the surface normal, now pointing outwards. Then one gets zero stress field outside, $p\hat{\boldsymbol{n}}$ on S_i, and the constant pressure field $2p\boldsymbol{\delta}$ as the stress field on the inside. If the fluid domain is bounded, having a container boundary surface, the single layers on the particles will not affect on S_c according to the above, and so the eigenvalue must be -1. If there is no container, the eigenvalue is similarly deduced to be 1, since the particles do not affect each other with these densities (see Exercise 17.13). Thus *an eigenfunction with* $\lambda \neq \pm 1$ *necessarily induces nonzero (positive) dissipation in the whole space.*

Let ψ now be a complex eigenfunction of $\mathcal{K}^*$, satisfying

$$0 = -\lambda\psi + \mathcal{K}^*\psi \ , \tag{17.3}$$

where $\lambda \neq \pm 1$. On denoting the LHSs of Equations 15.17 by $\boldsymbol{T}_{(i)}$ and $\boldsymbol{T}_{(e)}$, it is found that

$$2\psi = \boldsymbol{T}_{(e)} - \boldsymbol{T}_{(i)} \tag{17.4}$$

$$2\mathcal{K}^*\psi = \boldsymbol{T}_{(e)} + \boldsymbol{T}_{(i)} \ . \tag{17.5}$$

Substitute these into 17.3 to get

$$0 = (1-\lambda)\boldsymbol{T}_{(e)} + (1+\lambda)\boldsymbol{T}_{(i)}. \tag{17.6}$$

Note also that the energy equation 14.14 gives the dissipations

$$\left.\begin{aligned} D_{(i)} &= 2\mu \int_{Q_{(i)}} \boldsymbol{e}{:}\boldsymbol{e}^c \, dQ = \ -\oint_S \boldsymbol{T}_{(i)} \cdot \boldsymbol{V}^c \, dS \\ D_{(e)} &= 2\mu \int_{Q_{(e)}} \boldsymbol{e}{:}\boldsymbol{e}^c \, dQ = \ \oint_S \boldsymbol{T}_{(e)} \cdot \boldsymbol{V}^c \, dS \end{aligned}\right\} \ , \tag{17.7}$$

where the continuity of $\boldsymbol{V}$ across the boundary was used. The sign change is due to using the normal $\hat{\boldsymbol{n}}$ pointing into $Q_{(i)}$ in all equations. Multiply the first equation by $-(1+\lambda)$ and the second by $1-\lambda$ before adding; then the surface integrals cancel according to Equation 17.6 and

$$-(1+\lambda)D_{(i)} + (1-\lambda)D_{(e)} = 0 \; . \tag{17.8}$$

Taking the imaginary part of this equation gives

$$\Im(\lambda)\left(D_{(i)} + D_{(e)}\right) = 0 \; . \tag{17.9}$$

Since the total dissipation is a positive real number, λ must be real. Going back to the previous equation, solving for λ gives

$$\lambda = \left(D_{(e)} - D_{(i)}\right) / \left(D_{(e)} + D_{(i)}\right) \; , \tag{17.10}$$

where the division is allowed for $\lambda \neq \pm 1$, and this shows that $\lambda \in [-1, 1]$, since the dissipations are non-negative.

Odqvist referred to Plemelj's work, presumably on electrostatic problems, in connection with the proof of the spectrum being real. He did not consider complex Stokes solutions, as is done here, and also otherwise the treatment here is more detailed, but it is most likely that the proof he had in mind was along the spirit of the one presented here. In the next two subsections, we derive the spectrum for the single-sphere and for the two-sphere system. In both cases, we obtain analytic results for the spectrum that illustrate the salient points of the general theory.

17.2.1 The Spectrum for the Sphere

For a sphere, the eigenfunctions can be obtained by using Lamb's solution for the interior and exterior flows, and applying the jump conditions across a double layer distribution. Suppose that $\boldsymbol{\varphi}$ is an eigenfunction of the double layer operator, *i.e.*,

$$\int_S \boldsymbol{K}(\boldsymbol{\eta}, \boldsymbol{\xi}) \cdot \boldsymbol{\varphi}(\boldsymbol{\xi}) \, dS(\boldsymbol{\xi}) \;=\; \lambda \boldsymbol{\varphi}(\boldsymbol{\eta}) \; .$$

The flow fields outside and inside the particle then satisfy the following conditions at the particle surface:

$$\begin{aligned} \boldsymbol{\varphi} + \mathcal{K}(\boldsymbol{\varphi}) \;&=\; (\lambda+1)\boldsymbol{\varphi} \;=\; \boldsymbol{v}^{(o)} \\ -\boldsymbol{\varphi} + \mathcal{K}(\boldsymbol{\varphi}) \;&=\; (\lambda-1)\boldsymbol{\varphi} \;=\; \boldsymbol{v}^{(i)} \; . \end{aligned}$$

Therefore, it follows that $\boldsymbol{\varphi}$ is an eigenfunction of the double layer operator if and only if it satisfies the jump conditions,

$$\boldsymbol{\sigma}^{(o)} \cdot \hat{\boldsymbol{n}} \;=\; \boldsymbol{\sigma}^{(i)} \cdot \hat{\boldsymbol{n}} \qquad \text{and} \qquad \boldsymbol{v}^{(i)} \;=\; \kappa \boldsymbol{v}^{(o)} \; ,$$

with κ defined as $\kappa = (\lambda - 1)/(\lambda + 1)$. The first condition is the usual statement that tractions are continuous across a double layer distribution; the second

condition says that the velocity discontinuity takes a special form for eigenfunctions.

It turns out that the toroidal field, $\nabla \times (\boldsymbol{x}\chi)$, decouples from the other problems, so that we may break the task at hand into two smaller subproblems. On the unit sphere, the velocity field $\nabla \times (\boldsymbol{x}\chi_n) = -\boldsymbol{x} \times \nabla\chi_n$ has the surface traction (Chapter 4)

$$\boldsymbol{\sigma} \cdot \hat{\boldsymbol{n}} \;=\; \mu(n-1)\nabla \times (\boldsymbol{x}\chi_n)$$

for both positive n (interior flows) and negative n (exterior flows). The exterior and interior surface tractions match if we apply the usual correspondence between n and $-n-1$. For example, for axisymmetric problems $m = 0$, if the harmonics χ_n are written as $c_n r^n P_n$ and $C_n r^{-n-1} P_n$, we have

$$\begin{aligned} \boldsymbol{\sigma}^{(i)} \cdot \hat{\boldsymbol{n}} &= -c_n \mu(n-1)\boldsymbol{e}_\phi \frac{\partial P_n}{\partial \theta} \\ \boldsymbol{\sigma}^{(o)} \cdot \hat{\boldsymbol{n}} &= C_n \mu(n+2)\boldsymbol{e}_\phi \frac{\partial P_n}{\partial \theta} \,. \end{aligned}$$

Matching of surface tractions implies

$$c_n(n-1) \;+\; C_n(n+2) \;=\; 0 \,,$$

while the jump condition for the velocity fields requires

$$\boldsymbol{x} \times \nabla\chi_n \;=\; \kappa \boldsymbol{x} \times \nabla\chi_{-n-1}$$

or

$$c_n \;=\; \kappa_n C_n \,.$$

The system of equations for c_n and C_n has a nontrivial solution if and only if the determinant vanishes, which implies that

$$\kappa_n \;=\; -\frac{n+2}{n-1} \,.$$

The eigenvalues follow from the definition of κ_n as

$$\lambda_n \;=\; \frac{1+\kappa_n}{1-\kappa_n} \;=\; \frac{-3}{2n+1} \,, \qquad n = 1, 2, 3, \ldots \,.$$

The first few eigenvalues are -1, $-3/5$, $-3/7, \ldots$, with -1 corresponding to rigid-body rotation about the z-axis, as required by the general theory. It is also easy to show that eigenfunctions are also obtained starting from the more general form for χ_n involving $P_n^m e^{im\phi}$, $0 \le |m| \le n$, so that λ_n has multiplicity $2n+1$, with the corresponding eigenfunctions,

$$(1+\lambda_n)^{-1} \nabla \times (\boldsymbol{x}\chi_n)|_{r=1} \,.$$

The factor of $(1+\lambda_n)^{-1}$ was introduced here to make the velocity generated by the double layer equal to $\nabla \times (\boldsymbol{x}\chi_n)$. Note also that this velocity field is proportional to the orthogonal basis function, $\boldsymbol{\varphi}^{(3)}$, of Chapter 4.

We now turn our attention to the pressure and $\nabla\Phi$ terms in Lamb's solution. Again, consider axisymmetric fields first. Suppose that the interior and exterior velocity fields are given by

$$\begin{aligned}
\boldsymbol{v}^{(i)} &= b_n\nabla\Phi_n + a_n\left\{\frac{(n+3)r^2\nabla p_n}{2(n+1)(2n+3)} - \frac{n\boldsymbol{x}p_n}{(n+1)(2n+3)}\right\} \\
\boldsymbol{v}^{(o)} &= B_n\nabla\Phi_{-n-1} + A_n\left\{-\frac{(n-2)r^2\nabla p_{-n-1}}{2n(2n-1)} + \frac{(n+1)\boldsymbol{x}p_{-n-1}}{n(2n-1)}\right\} .
\end{aligned}$$

Then on the unit sphere, the surface tractions are (Chapter 4)

$$\begin{aligned}
\frac{\boldsymbol{\sigma}^{(i)}\cdot\hat{\boldsymbol{n}}}{\mu} &= b_n 2(n-1)\nabla\Phi_n + a_n\left\{-\frac{(2n^2+4n+3)}{(n+1)(2n+3)}\boldsymbol{x}p_n + \frac{n(n+2)r^2\nabla p_n}{(n+1)(2n+3)}\right\} \\
&= \boldsymbol{e}_r P_n\left\{b_n 2n(n-1) + a_n\frac{(n^2-n-3)}{(2n+3)}\right\} \\
&\quad + \boldsymbol{e}_\theta\frac{\partial P_n}{\partial\theta}\left\{b_n 2(n-1) + a_n\frac{n(n+2)}{(n+1)(2n+3)}\right\} \\
\frac{\boldsymbol{\sigma}^{(o)}\cdot\hat{\boldsymbol{n}}}{\mu} &= -B_n 2(n+2)\nabla\Phi_{-n-1} \\
&\quad + A_n\left\{-\frac{(2n^2+1)}{n(2n-1)}\boldsymbol{x}p_{-n-1} + \frac{(n+1)(n-1)}{n(2n-1)}r^2\nabla p_{-n-1}\right\} \\
&= \boldsymbol{e}_r P_n\left\{B_n 2(n+1)(n+2) - A_n\frac{(n^2+3n-1)}{(2n-1)}\right\} \\
&\quad + \boldsymbol{e}_\theta\frac{\partial P_n}{\partial\theta}\left\{-B_n 2(n+2) + A_n\frac{(n+1)(n-1)}{n(2n-1)}\right\}
\end{aligned}$$

and matching implies that

$$2n(n-1)b_n + \frac{(n^2-n-3)}{(2n+3)}a_n - 2(n+1)(n+2)B_n + \frac{(n^2+3n-1)}{(2n-1)}A_n = 0 \quad (17.11)$$

$$2(n-1)b_n + \frac{n(n+2)}{(n+1)(2n+3)}a_n + 2(n+2)B_n - \frac{(n+1)(n-1)}{n(2n-1)}A_n = 0 . \quad (17.12)$$

The relation $\boldsymbol{v}^{(i)} = \kappa\boldsymbol{v}^{(o)}$ provides two more equations (from the r and θ components):

$$nb_n + \frac{n}{2(2n+3)}a_n + \kappa(n+1)B_n - \kappa\frac{(n+1)}{2(2n-1)}A_n = 0 \quad (17.13)$$

$$b_n + \frac{(n+3)}{2(n+1)(2n+3)}a_n - \kappa B_n + \kappa\frac{(n-2)}{2n(2n-1)}A_n = 0 . \quad (17.14)$$

The problem thus reduces to finding κ such that

$$\begin{vmatrix}
2n(n-1) & \frac{n^2-n-3}{2n+3} & -2(n+2)(n+1) & \frac{n^2+3n-1}{2n-1} \\
2(n-1) & \frac{n(n+2)}{(n+1)(2n+3)} & 2(n+2) & -\frac{(n+1)(n-1)}{n(2n-1)} \\
n & \frac{n}{2(2n+3)} & (n+1)\kappa & -\frac{(n+1)}{2(2n-1)}\kappa \\
1 & \frac{n+3}{2(n+1)(2n+3)} & -\kappa & \frac{(n-2)}{2n(2n-1)}\kappa
\end{vmatrix} = 0 .$$

This is a quadratic equation for κ. Note that the determinant is invariant with respect to the operation of replacing n and κ by $-n-1$ and $1/\kappa$, because of the corresponding relationship between the interior and exterior fields in Lamb's general solution. Therefore, if $\kappa(n)$ is a root, then so is $1/\kappa(-n-1)$.

After expansion of the determinant, we obtain the quadratic equation explicitly,

$$\kappa^2 + \frac{8n^4+16n^3+4n^2-4n+3}{2(n^2-1)(2n^2+4n+3)}\kappa + \frac{n(n+2)(2n^2+1)}{(n^2-1)(2n^2+4n+3)} = 0$$

or

$$\kappa^2 + \left[2+\frac{3(4n+5)}{2(n^2-1)(2n^2+4n+3)}\right]\kappa + \left[1+\frac{3(2n+1)}{(n^2-1)(2n^2+4n+3)}\right] = 0\,.$$

The discriminant of this quadratic equation,

$$\frac{16n^4+32n^3+24n^2+8n+1}{4(n^2-1)^2(2n^2+4n+3)^2} = \frac{(2n+1)^4}{4(n^2-1)^2(2n^2+4n+3)^2}\,,$$

is a perfect square, and the roots turn out to be

$$\kappa_n^{\pm} = -1+\frac{3}{4}\left[\frac{-(4n+5)\pm(2n+1)^2}{(n^2-1)(2n^2+4n+3)}\right]\,.$$

We may simplify this further as

$$\begin{aligned}\kappa_n^- &= -\frac{2n^2+1}{2(n^2-1)}\\ \kappa_n^+ &= -\frac{2n(n+2)}{2n^2+4n+3}\,,\end{aligned}$$

and we see that the two branches do indeed satisfy the relation,

$$\kappa_{-(n+1)}^- = \kappa_{n+1}^- = \frac{1}{\kappa_n^+}\,,$$

as stated earlier. The corresponding eigenvalues are found to be

$$\begin{aligned}\lambda_n^- &= \frac{1+\kappa_n^-}{1-\kappa_n^-} = \frac{-3}{(2n-1)(2n+1)}\,, \qquad \text{for } n=1,2,3,\ldots\\ \lambda_n^+ &= \frac{1+\kappa_n^+}{1-\kappa_n^+} = \frac{3}{(2n+1)(2n+3)}\,, \qquad \text{for } n=0,1,2,\ldots\,.\end{aligned}$$

The two eigenvalue branches satisfy the relation,

$$\lambda_{n+1}^- = -\lambda_n^+\,, \qquad \text{for } n=0,1,2,\ldots\,.$$

The first few are ± 1, $\pm 1/5$, $\pm 3/35$, $\pm 1/21$, $\pm 1/33$, ...

As before, the nonaxisymmetric case follows the same structure, so that the degeneracy of the eigenvalue $\lambda_n^{\pm}$ is $(2n+1)$. Note that the matched pair λ_{n+1}^- and λ_n^+ have different multiplicities, *viz.*, $2n+3$ and $2n+1$, respectively. For $n=0$, we already know from the general theory that there are three translational null functions ($\lambda=-1$) and one container null function ($\lambda=1$). This analysis also confirms the obvious result that for a sphere, the container null function is in fact the surface normal.

The five eigenfunctions with $\lambda_2^- = -1/5$ correspond to a sphere in a rate-of-strain field, $\boldsymbol{v}^\infty = \boldsymbol{E}\cdot\boldsymbol{x}$, of which there are five linearly independent fields. These, in fact, were encountered in Section 16.3 in the discussion of the sphere in a rate-of-strain field. The three eigenfunctions with $\lambda_2^+ = 1/5$ correspond to the degenerate quadrupole, $\boldsymbol{F}\cdot\nabla^2\mathcal{G}(\boldsymbol{\xi})$, which we also encountered in Section 16.3.

We turn our attention to the general description of the eigenfunctions. We assume that κ is appropriately chosen so that the system of equations, 17.11–17.14, has a nontrivial solution. We discard 17.11 and use pairings 17.13 and 17.14, as well as 17.12 and 17.14, to obtain two independent equations without the b_ns:

$$(2n+1)\kappa B_n - \frac{\kappa}{2}A_n = \frac{n a_n}{(n+1)(2n+3)}$$

$$\{2\kappa(n-1)+2(n+2)\}\,B_n - \frac{(n-1)\,(\kappa(n-2)+n+1)}{n(2n-1)}A_n = \frac{-3a_n}{(n+1)(2n+3)}\,.$$

We may eliminate a_n from these equations to obtain

$$\left[\kappa(2n^2+4n+3)+2n(n+2)\right]B_n = \frac{\kappa(2n^2+1)+2(n-1)(n+1)}{2(2n-1)}A_n\,. \tag{17.15}$$

If we use $\kappa=\kappa_n^+$, then the nontrivial solution can be chosen as $A_n=0$ and $B_n=1$, and the eigenfunctions φ_n^+, proportional to

$$\nabla\Phi_{-n-1}|_{r=1}\,, \qquad \text{with} \quad \lambda_n^+ = \frac{3}{(2n+1)(2n+3)}\,,$$

for $n\geq 0$ are obtained. On the other hand, if we use $\kappa=\kappa_n^-$, then Equation 17.15 simplifies to

$$B_n = \frac{1}{2(2n+1)}A_n\,.$$

These eigenfunctions, which we denote as φ_n^-, are of the form,

$$\left\{-\frac{(n-2)r^2\nabla p_{-n-1}}{2n(2n-1)} + \frac{(n+1)\boldsymbol{x}p_{-n-1}}{n(2n-1)}\right\}|_{r=1} + \frac{\nabla p_{-n-1}|_{r=1}}{2(2n+1)}\,,$$

and the associated eigenvalues are

$$\lambda_n^- = -\frac{3}{(2n-1)(2n+1)}\,.$$

The eigenfunctions may also be written in terms of interior fields. With the above relation between A_n and B_n, we find that $a_n = 0$, so that only the b_n term survives. Therefore, the eigenfunction φ_n^- is also proportional to $\nabla(r^n P_n)|_{r=1}$.

Using the relations between Lamb's general solution and the multipole expansion (Chapter 4), we may *define* φ_n^+ and φ_n^- as

$$(1+\lambda_n^+)\varphi_n^+ = \boldsymbol{P}^{(n-1)} \cdot \nabla^2 \mathcal{G}|_{r=1} \tag{17.16}$$

$$(1+\lambda_n^-)\varphi_n^- = \boldsymbol{P}^{(n-1)} \cdot \left\{ 1 + \frac{1}{2(2n+1)} \nabla^2 \right\} \mathcal{G}|_{r=1} - \frac{\boldsymbol{P}^{(n-3)} \cdot \mathcal{G}|_{r=1}}{2(2n-1)} , \tag{17.17}$$

where $\boldsymbol{P}^{(n)}$ is the vector differential operator that gives an n-th multipole. As double layer densities, the eigenfunctions $\varphi_n^{\pm}$ generate outside the sphere the velocity fields on the RHS of Equations 17.16 and 17.17. For $\lambda_1^- = -1$, Equation 17.17 should be interpreted as the RBM translational null function generating zero velocity outside the sphere.

The multipole expansion for axisymmetric flows (symmetry axis $\boldsymbol{d} = -\boldsymbol{e}_z$) past a sphere,

$$\boldsymbol{v} = \sum_{n=0}^{\infty} \left\{ A_n \frac{(\boldsymbol{d}\cdot\nabla)^n}{n!} \boldsymbol{d} \cdot \mathcal{G} + B_n \frac{(\boldsymbol{d}\cdot\nabla)^n}{n!} \boldsymbol{d} \cdot \nabla^2 \mathcal{G} \right\} ,$$

may also be written as a completed double layer representation,

$$\boldsymbol{v} = A_0 \boldsymbol{d} \cdot \mathcal{G} + \oint_S \boldsymbol{K}(\boldsymbol{x}, \boldsymbol{\xi}) \cdot \boldsymbol{\varphi}(\boldsymbol{\xi}) \, dS ,$$

with the double layer density on the sphere surface expanded as

$$\boldsymbol{\varphi}(\boldsymbol{\xi}) = \sum_{n=1}^{\infty} \alpha_n \boldsymbol{\varphi}_{n+1}^-(\boldsymbol{\xi}) + \sum_{n=0}^{\infty} \beta_n \boldsymbol{\varphi}_{n+1}^+(\boldsymbol{\xi}) .$$

Using this result, we may express many of the results from Parts II and III with the completed double layer representation, thereby expanding our knowledge of analytic solutions for CDL-BIEM. In particular, the image for a Stokeslet near a fixed rigid sphere may be expressed as a combination of a Stokeslet inside the sphere plus a double layer density on the sphere surface. The "smoothness" of the double layer density depends on the location of the Stokeslet inside the sphere, thus providing an instructive example of the importance of selecting a good basis for completing the range (see the exercises).

We conclude the discussion by noting that $\mathcal{K}$ is self-adjoint for the sphere, *i.e.*, $K_{ij}(\boldsymbol{\eta}, \boldsymbol{\xi}) = K_{ji}(\boldsymbol{\xi}, \boldsymbol{\eta})$. This result follows from, among other things,

$$\hat{\boldsymbol{n}}(\boldsymbol{\xi}) \cdot (\boldsymbol{\eta} - \boldsymbol{\xi}) = -\hat{\boldsymbol{n}}(\boldsymbol{\eta}) \cdot (\boldsymbol{\eta} - \boldsymbol{\xi}) ,$$

a condition satisfied for points $\boldsymbol{\xi}$ and $\boldsymbol{\eta}$ on a sphere. It then follows that the eigenfunctions of the double layer operator are orthogonal. This is the underlying principle behind the orthogonal properties of the orthonormalized basis of

Chapter 4:

$$\varphi^{(1)}_{nm}(\xi) = \sqrt{n(2n+1)}\frac{(2n-1)}{\eta_{nm}(n+1)} \times \left\{ -\frac{(n-2)r^2\nabla}{2n(2n-1)} + \frac{(n+1)\boldsymbol{x}}{n(2n-1)} + \frac{\nabla}{2(2n+1)} \right\} \left\{ r^{-n-1}\widetilde{Y}^m_n \right\} \tag{17.18}$$

$$= \frac{\sqrt{n(2n+1)}}{\eta_{nm}} \left[\frac{r^{-n}\boldsymbol{A}_{nm}}{n(2n+1)} + \frac{(2n-1)}{(2n+1)} \frac{(r^{-2}-1)\, r^{-n}\boldsymbol{B}_{nm}}{2(n+1)} \right]$$

$$\varphi^{(2)}_{nm} = \frac{\nabla \left\{ r^{-n-1}\widetilde{Y}^m_n \right\}}{\eta_{nm}\sqrt{(n+1)(2n+1)}} = \frac{r^{-n-2}\boldsymbol{B}_{nm}}{\eta_{nm}\sqrt{(n+1)(2n+1)}} \tag{17.19}$$

$$\varphi^{(3)}_{nm} = \frac{i}{\eta_{nm}\sqrt{n(n+1)}} \nabla \times \left\{ \boldsymbol{x} r^{-n-1}\widetilde{Y}^m_n \right\} = \frac{i r^{-n-1}\boldsymbol{C}_{nm}}{\eta_{nm}\sqrt{n(n+1)}}, \tag{17.20}$$

all evaluated at $r = 1$. The associated eigenvalues are $-3/(2n-1)(2n+1)$ $(n \geq 1)$, $3/(2n+1)(2n+3)$ $(n \geq 0)$, and $-3/(2n+1)$ $(n \geq 1)$, respectively.

It is also now clear why the canonical solution in the translation problem (Section 16.3) was simply a degenerate quadrupole evaluated at the sphere surface – the degenerate quadrupole "generates itself," since it is an eigenfunction, and it is orthogonal to the null functions since those are eigenfunctions too.

17.2.2 Double Layer Eigenfunctions for Ellipsoids in Rate-of-Strain Fields

This section emphasizes the fact that only the extreme eigenvalues at $\lambda = \pm 1$ (associated with the null functions) are universal (independent of particle shape). The specific analytical example considered here is the eigenvalues/eigenfunctions corresponding to the disturbance fields for an ellipsoid in the rate-of-strain fields, $\boldsymbol{E} \cdot \boldsymbol{x}$. For the sphere we just saw that only the eigenvalue $-1/5$ comes up in this way, so that there are five independent eigenfunctions corresponding to it. For the general ellipsoid this degeneracy disappears, and we shall discover five eigenfunctions with, in general, different eigenvalues. We will inspect how these eigenvalues change continuously with the shape parameters of the ellipsoid.

As before, we pick our coordinate system so that the ellipsoid is described by the equation,

$$\frac{x^2}{a^2} + \frac{y^2}{b^2} + \frac{z^2}{c^2} = 1 ,$$

with $a \geq b \geq c > 0$. We will show that the linear field $\boldsymbol{E} \cdot \xi$, $\xi \in S$ is an eigenfunction of the double layer operator on the ellipsoidal surface, with $\boldsymbol{E}$ corresponding physically to a constant rate-of-strain tensor.

We decompose the rate-of-strain tensor as follows:

$$\begin{pmatrix} E_{11} & E_{12} & E_{13} \\ E_{21} & E_{22} & E_{23} \\ E_{31} & E_{32} & E_{33} \end{pmatrix} = \begin{pmatrix} 0 & E_{12} & 0 \\ E_{21} & 0 & 0 \\ 0 & 0 & 0 \end{pmatrix} + \begin{pmatrix} 0 & 0 & E_{13} \\ 0 & 0 & 0 \\ E_{31} & 0 & 0 \end{pmatrix}$$

$$+ \begin{pmatrix} 0 & 0 & 0 \\ 0 & 0 & E_{23} \\ 0 & E_{32} & 0 \end{pmatrix} + \begin{pmatrix} E_{11} & 0 & 0 \\ 0 & E_{22} & 0 \\ 0 & 0 & E_{33} \end{pmatrix} ,$$

with $E_{11} + E_{22} + E_{33} = 0$. In the following, we denote these rate-of-strain fields as $\boldsymbol{E}^{(1)}, \ldots, \boldsymbol{E}^{(4)}$. We first consider the "off-diagonal" cases involving ($\boldsymbol{E}^{(1)}$, $\boldsymbol{E}^{(2)}$, $\boldsymbol{E}^{(3)}$).

Off-Diagonal Rate-of-Strain Fields

Our strategy is to construct velocity fields outside and inside the ellipsoid, with matching traction fields. The double layer density is one-half of the velocity jump, and if it is also proportional to the outer and inner fields evaluated at the ellipsoid surface, then we have an eigenfunction.

Consider the rate-of-strain field,

$$\boldsymbol{E}^{(1)} = \begin{pmatrix} 0 & E_{12} & 0 \\ E_{21} & 0 & 0 \\ 0 & 0 & \end{pmatrix} ,$$

immerse in it a torque-free ellipsoid rotating about the z-axis with the rotational velocity,

$$\omega_3 = \left(\frac{a^2 - b^2}{a^2 + b^2} \right) E_{12} .$$

The disturbance field of this force-free, torque-free ellipsoid can be represented by the double layer alone. From Jeffery's classical paper (see also Chapter 3), we have the following simple result for the tractions *on the ellipsoid surface*:

$$\boldsymbol{\sigma}^{(o)} \cdot \hat{\boldsymbol{n}} = \left[\frac{4\mu}{\gamma_0'(a^2 + b^2)} - 2\mu \right] \boldsymbol{E}^{(1)} \cdot \hat{\boldsymbol{n}} .$$

We have followed the definition,

$$\gamma_0' = abc \int_0^\infty \frac{dt}{(a^2 + t)(b^2 + t)\Delta(t)} ,$$

which differs from Jeffery's by the factor of (abc).

This surface traction is matched inside the ellipsoid by the linear velocity field,

$$\boldsymbol{v}^{(i)} = \left[\frac{2}{\gamma_0'(a^2 + b^2)} - 1 \right] \boldsymbol{E}^{(1)} \cdot \boldsymbol{x} ,$$

and the double layer density can be determined immediately from

$$2\boldsymbol{\varphi} = \boldsymbol{v}^{(o)} - \boldsymbol{v}^{(i)} = \left[-\boldsymbol{E}^{(1)} \cdot \boldsymbol{\xi} + \boldsymbol{\omega} \times \boldsymbol{\xi} \right] - \left[\frac{2}{\gamma_0'(a^2 + b^2)} - 1 \right] \boldsymbol{E}^{(1)} \cdot \boldsymbol{\xi} .$$

The rotatonal motion is a null solution and generates no flow, so we may drop it. Or equivalently, we could put the same RBM rotation inside the particle, a

flow that generates no traction, and then the expression for the velocity jump (= 2φ) would not involve angular velocities at all. We thus arrive at the conclusion that the double layer density is given by

$$\varphi = -\frac{\boldsymbol{E}^{(1)} \cdot \boldsymbol{\xi}}{\gamma_0'(a^2+b^2)} ,$$

and is proportional to $\boldsymbol{v}^{(i)}$ and $\boldsymbol{v}^{(o)}$. Therefore, $\boldsymbol{E}^{(1)} \cdot \boldsymbol{\xi}$ is an eigenfunction. The eigenvalue follows from

$$\lambda = \frac{1+\kappa}{1-\kappa} , \qquad \text{with} \qquad \boldsymbol{v}^{(i)} = \kappa \boldsymbol{v}^{(o)} .$$

Since this eigenvalue is associated with E_{12} and E_{21}, we denote it as $\lambda^{(12)}$.

We determine κ from the expression for the inner and outer velocities, and the expressions for the eigenvalues follow from the preceding equations as

$$\begin{aligned} \lambda^{(12)} &= (a^2+b^2)\gamma_0' - 1 \\ \lambda^{(23)} &= (b^2+c^2)\alpha_0' - 1 \\ \lambda^{(31)} &= (c^2+a^2)\beta_0' - 1 , \end{aligned}$$

with the last two following by permutative symmetry. All three eigenvalues become equal to $-1/5$ when $a = b = c$, but for the general ellipsoid, they are nondegenerate. This completes the discussion of the eigenvalues associated with the off-diagonal rate-of-strain fields.

Diagonal Rate-of-Strain Fields

Consider the rate-of-strain field,

$$\begin{pmatrix} E_{11} & 0 & 0 \\ 0 & E_{22} & 0 \\ 0 & 0 & E_{33} \end{pmatrix} ,$$

with $E_{11} + E_{22} + E_{33} = 0$. Jeffery defines the constants, A, B, and C by

$$\begin{aligned} A &= \frac{1}{6} \frac{2\alpha_0'' E_{11} - \beta_0'' E_{22} - \gamma_0'' E_{33}}{\beta_0''\gamma_0'' + \gamma_0''\alpha_0'' + \alpha_0''\beta_0''} \\ B &= \frac{1}{6} \frac{2\beta_0'' E_{22} - \gamma_0'' E_{33} - \alpha_0'' E_{11}}{\beta_0''\gamma_0'' + \gamma_0''\alpha_0'' + \alpha_0''\beta_0''} \\ C &= \frac{1}{6} \frac{2\gamma_0'' E_{33} - \alpha_0'' E_{11} - \beta_0'' E_{22}}{\beta_0''\gamma_0'' + \gamma_0''\alpha_0'' + \alpha_0''\beta_0''} \end{aligned}$$

and shows that on the ellipsoid surface the tractions of the disturbance field simplify to

$$\begin{aligned} (\boldsymbol{\sigma} \cdot \hat{\boldsymbol{n}})_x &= [8\mu A - 2\mu E_{11} - 4\mu(\alpha_0 A + \beta_0 B + \gamma_0 C)]\, n_x \\ (\boldsymbol{\sigma} \cdot \hat{\boldsymbol{n}})_y &= [8\mu B - 2\mu E_{22} - 4\mu(\alpha_0 A + \beta_0 B + \gamma_0 C)]\, n_y \\ (\boldsymbol{\sigma} \cdot \hat{\boldsymbol{n}})_z &= [8\mu C - 2\mu E_{33} - 4\mu(\alpha_0 A + \beta_0 B + \gamma_0 C)]\, n_z . \end{aligned}$$

Again, Jeffery's expression for the traction differs from ours (the first terms on the RHSs of the above equations) because of the factor of (abc) difference in the definitions of the elliptic integrals.

The traction field is of the form,

$$\boldsymbol{\sigma}^{(o)} \cdot \hat{\boldsymbol{n}} = 2\mu \boldsymbol{D} \cdot \hat{\boldsymbol{n}} - 2\mu \boldsymbol{E}^{(4)} \cdot \hat{\boldsymbol{n}} \; - \; 4\mu(\alpha_0 A + \beta_0 B + \gamma_0 C)\hat{\boldsymbol{n}} \; ,$$

with

$$\boldsymbol{D} = \begin{pmatrix} 4A & 0 & 0 \\ 0 & 4B & 0 \\ 0 & 0 & 4C \end{pmatrix} .$$

The constant pressure may be dropped from further consideration, because it is not used at all in the expression for the interior field,

$$\boldsymbol{v}^{(i)} \; = \; \boldsymbol{D} \cdot \boldsymbol{x} - \boldsymbol{E}^{(4)} \cdot \boldsymbol{x} \; .$$

We now set the condition, $\boldsymbol{v}^{(i)} = \kappa \boldsymbol{v}^{(o)}$, which leads to

$$4A \; = \; (1-\kappa)E_{11} \; , \qquad 4B \; = \; (1-\kappa)E_{22} \; , \qquad 4C \; = \; (1-\kappa)E_{33} \; .$$

We insert the expressions for A, B, and C to arrive at the following system of equations:

$$\begin{aligned} \left[(\kappa-1) + \frac{4\alpha_0''}{3d}\right] E_{11} - \frac{2\beta_0''}{3d} E_{22} - \frac{2\gamma_0''}{3d} E_{33} \; &= \; 0 \\ -\frac{2\alpha_0''}{3d} E_{11} \left[(\kappa-1) + \frac{4\beta_0''}{3d}\right] E_{22} - \frac{2\gamma_0''}{3d} E_{33} \; &= \; 0 \\ -\frac{2\alpha_0''}{3d} E_{11} - \frac{2\beta_0''}{3d} E_{22} + \left[(\kappa-1) + \frac{4\gamma_0''}{3d}\right] E_{33} \; &= \; 0 \; . \end{aligned}$$

Note, however, that $E_{11} + E_{22} + E_{33} = 0$, and so these three variables and the three equations are not independent. Under these circumstances, κ is determined by taking any two equations from the preceding set of three, plus the zero-trace condition, $E_{11} + E_{22} + E_{33} = 0$. The problem thus reduces to finding κ such that

$$\begin{vmatrix} (\kappa-1) + \frac{4\alpha_0''}{3d} & -\frac{2\beta_0''}{3d} & -\frac{2\gamma_0''}{3d} \\ -\frac{2\alpha_0''}{3d} & (\kappa-1) + \frac{4\beta_0''}{3d} & -\frac{2\gamma_0''}{3d} \\ 1 & 1 & 1 \end{vmatrix} \; = \; 0 \; .$$

After expansion of the determinant, we obtain the quadratic equation,

$$(\kappa-1)^2 \; + \; \frac{4}{3d}(\alpha_0'' + \beta_0'' + \gamma_0'')(\kappa-1) \; + \; \frac{4}{3d} \; = \; 0 \; ,$$

with roots

$$\kappa^{\pm} \; = \; 1 - \frac{2}{3d}(\alpha_0'' + \beta_0'' + \gamma_0'') \pm \frac{2}{3d}\sqrt{[\alpha_0'']^2 + [\beta_0'']^2 + [\gamma_0'']^2 - d} \; ,$$

and the *two* eigenvalues follow as

$$\lambda^{\pm} \; = \; \frac{1+\kappa^{\pm}}{1-\kappa^{\pm}} \; .$$

We now consider further simplifications of these results as applied to ellipsoids of revolution.

Prolate Spheroids

We set $a \geq b = c$, then the eigenvalues from the off-diagonal case simplify to

$$\begin{aligned} \lambda^{(12)} = \lambda^{(31)} &= (a^2 + c^2)\gamma_0' - 1 \\ \lambda^{(23)} &= 2c^2\alpha_0' - 1 \,, \end{aligned}$$

while the eigenvalues from the diagonal rate-of-strain field reduce to

$$\begin{aligned} \lambda^- &= -1 + 3\gamma_0'' \\ \lambda^+ &= -1 + 2\alpha_0'' + \gamma_0'' \,. \end{aligned}$$

The rate-of-strain field for the eigenvalue λ^- corresponds to uniaxial extension along the x-axis (an axisymmetric flow about the x-axis), while that for $\lambda^+ = \lambda^{(23)}$ corresponds to two-dimensional hyperbolic flow in the yz-plane. Thus as expected, for a prolate spheroid there are three distinct eigenvalues. If the shape of the spheroid is specified by the eccentricity, $e = \sqrt{a^2 - c^2}/a$, of the generating ellipse, then the relevant elliptic integrals simplify to (see Chapter 3):

$$\begin{aligned} \alpha_0' &= \frac{1}{a^2 8e^5(1-e^2)}\left[2(5e^3 - 3e) + 3(1-e^2)^2 \log\left(\frac{1+e}{1-e}\right)\right] \\ \gamma_0' &= \frac{1}{a^2 e^5}\left[3e - 2e^3 - \frac{3}{2}(1-e^2)\log\left(\frac{1+e}{1-e}\right)\right] \\ \alpha_0'' &= \frac{3-e^2}{4e^4} - \frac{(1-e^2)(e^2+3)}{8e^5}\log\left(\frac{1+e}{1-e}\right) \\ \gamma_0'' &= \frac{(1-e^2)}{e^5}\left[-3e + \frac{1}{2}(3-e^2)\log\left(\frac{1+e}{1-e}\right)\right] \,. \end{aligned}$$

The eigenvalues have the explicit expressions,

$$\begin{aligned} \lambda^{(12)} = \lambda^{(31)} &= -1 + \frac{(2-e^2)}{e^5}\left[3e - 2e^3 - \frac{3}{2}(1-e^2)\log\left(\frac{1+e}{1-e}\right)\right] \\ \lambda^{(23)} = \lambda^+ &= -1 + \frac{5e^2-3}{2e^4} + \frac{3(1-e^2)^2}{4e^5}\log\left(\frac{1+e}{1-e}\right) \\ \lambda^- &= -1 + \frac{3(1-e^2)}{e^5}\left[-3e + \frac{1}{2}(3-e^2)\log\left(\frac{1+e}{1-e}\right)\right] \,. \end{aligned}$$

The asymptotic behavior in the limit for near-spheres ($e \to 0$) are

$$\begin{aligned} \lambda^{(12)} = \lambda^{(31)} &\sim -\frac{1}{5} - \frac{2}{35}e^2 + \cdots \\ \lambda^{(23)} = \lambda^+ &\sim -\frac{1}{5} + \frac{4}{35}e^2 + \cdots \\ \lambda^- &\sim -\frac{1}{5} - \frac{4}{35}e^2 + \cdots \,. \end{aligned}$$

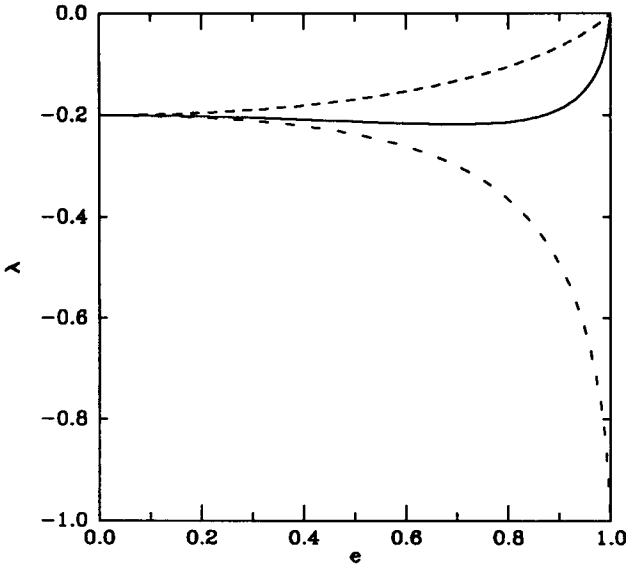

Figure 17.1: Eigenvalues for the prolate spheroid in a rate-of-strain field.

The asymptotic behavior in the slender-body limit ($e \to 1$) are

$$\begin{aligned} \lambda^{(12)} = \lambda^{(31)} &\sim \{-3\log(2\epsilon) + 5\}\,\epsilon^2 + \cdots \\ \lambda^{(23)} = \lambda^{+} &\sim -\frac{1}{2}\epsilon^2 + \cdots \\ \lambda^{-} &\sim -1 + \{6\log(2\epsilon) - 9\}\,\epsilon^2 + \cdots , \end{aligned}$$

with $\epsilon = c/a = \sqrt{1-e^2}$, the inverse of the aspect ratio. We see that the spectral radius of the deflated system must approach unity with increasing aspect ratio. The accompanying figure provides a plot of these eigenvalues *vs.* e.

Oblate Spheroids

We set $a = b > c$, then the eigenvalues from the off-diagonal case simplify to

$$\begin{aligned} \lambda^{(12)} &= 2a^2\gamma_0' - 1 \\ \lambda^{(23)} = \lambda^{(31)} &= (a^2 + c^2)\alpha_0' - 1 , \end{aligned}$$

while the eigenvalues from the diagonal rate-of-strain field reduce to

$$\begin{aligned} \lambda^{-} &= -1 + 3\alpha_0'' \\ \lambda^{+} &= -1 + \alpha_0'' + 2\gamma_0'' . \end{aligned}$$

The rate-of-strain field for the eigenvalue λ^{-} corresponds to uniaxial extension along the z-axis (an axisymmetric flow about the x-axis), while that for $\lambda^{+} =$

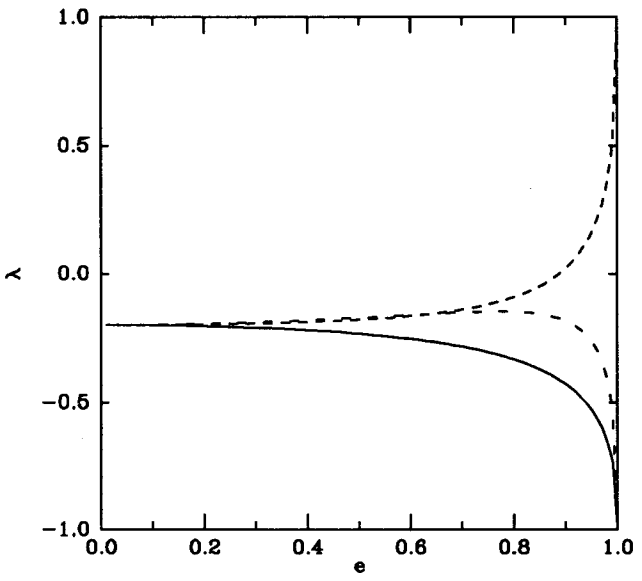

Figure 17.2: Eigenvalues for the oblate spheroid in a rate-of-strain field.

$\lambda^{(12)}$ corresponds to two-dimensional hyperbolic flow in the xy-plane, so again, as expected, there are three distinct eigenvalues. If the shape of the spheroid is specified by the eccentricity, $e = \sqrt{a^2 - c^2}/a$, of the generating ellipse, then the relevant elliptic integrals simplify to

$$\begin{aligned}
\alpha_0' &= \frac{1}{a^2}\left[\frac{3-e^2}{e^4} - \frac{3\sqrt{1-e^2}}{e^5}\cot^{-1}\left(\frac{\sqrt{1-e^2}}{e}\right)\right] \\
\gamma_0' &= \frac{1}{a^2}\left[\frac{(1-e^2)(e^2-3)}{4e^4} + \frac{3\sqrt{1-e^2}}{4e^5}\cot^{-1}\left(\frac{\sqrt{1-e^2}}{e}\right)\right] \\
\alpha_0'' &= -\frac{3(1-e^2)}{e^4} + \frac{(3-2e^2)\sqrt{1-e^2}}{e^5}\cot^{-1}\left(\frac{\sqrt{1-e^2}}{e}\right) \\
\gamma_0'' &= \frac{(1-e^2)(3-2e^2)}{4e^4} - \frac{(3-4e^2)\sqrt{1-e^2}}{4e^5}\cot^{-1}\left(\frac{\sqrt{1-e^2}}{e}\right) .
\end{aligned}$$

The eigenvalues have the explicit expressions

$$\begin{aligned}
\lambda^{(12)} = \lambda^{+} &= -1 - \frac{(1-e^2)(2e^2+3)}{2e^4} + \frac{3\sqrt{1-e^2}}{2e^5}\cot^{-1}\left(\frac{\sqrt{1-e^2}}{e}\right) \\
\lambda^{(23)} = \lambda^{(31)} &= -1 + (2-e^2)\left[\frac{3-e^2}{e^4} - \frac{3\sqrt{1-e^2}}{e^5}\cot^{-1}\left(\frac{\sqrt{1-e^2}}{e}\right)\right] \\
\lambda^{-} &= -1 - \frac{9(1-e^2)}{e^4} + \frac{3(3-2e^2)\sqrt{1-e^2}}{e^5}\cot^{-1}\left(\frac{\sqrt{1-e^2}}{e}\right) .
\end{aligned}$$

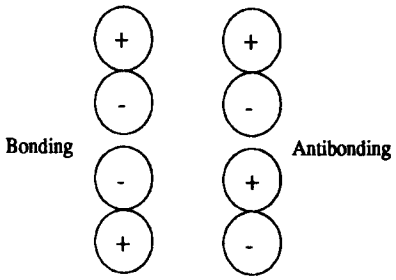

Figure 17.3: Bonding and anti-bonding combinations of p_z orbitals.

The asymptotic behavior in the limit for near-spheres ($e \to 0$) are

$$\begin{aligned} \lambda^{(12)} = \lambda^{+} &\sim -\frac{1}{5} - \frac{4}{35}e^2 + \cdots \\ \lambda^{(23)} = \lambda^{(31)} &\sim -\frac{1}{5} + \frac{2}{35}e^2 + \cdots \\ \lambda^{-} &\sim -\frac{1}{5} + \frac{4}{35}e^2 + \cdots . \end{aligned}$$

The asymptotic behavior in the thin-body limit ($e \to 1$) are

$$\begin{aligned} \lambda^{(12)} = \lambda^{+} &\sim -1 + \frac{3\pi}{4}\epsilon - 4\epsilon^2 + \cdots \\ \lambda^{(23)} = \lambda^{(31)} &\sim 1 - \frac{3\pi}{2}\epsilon + 10\epsilon^2 + \cdots \\ \lambda^{-} &\sim -1 + \frac{3\pi}{2}\epsilon - 12\epsilon^2 + \cdots , \end{aligned}$$

with $\epsilon = c/a = \sqrt{1-e^2}$, as before. We see that the spectral radius of the deflated system approaches unity, as the oblate spheroid is flattened, with eigenvalues approaching both ± 1, as shown in the figure. As expected, thin particles present a greater challenge.

17.2.3 The Spectrum for Two Spheres: HI-Induced Spectral Splitting

Consider two equal spheres with their centers $\boldsymbol{x}_1$, $\boldsymbol{x}_2$ separated by a distance $R = |\boldsymbol{x}_1 - \boldsymbol{x}_2|$. If R is very large, we may neglect interactions between the two and the eigensystem would simply be that obtained by superposition of the results for each sphere. The question is what happens as we decrease R.

At this point, it may be helpful to draw an analogy with a similar problem from quantum mechanics, *viz.*, the mixing of atomic orbitals to create molecular orbitals. For example, we can mix the p_z-orbitals of two widely separated atoms

in either a *bonding* $(\psi_1 - \psi_2)$ or *anti-bonding* $(\psi_1 + \psi_2)$ fashion. The former builds up electron densities in the overlap region, while the later creates an electron-deficient region near the newly created node.

With these ideas in mind, we write the eigenfunctions for the two-sphere system as

$$\varphi_n(1) = \varphi_n^{(0)}(1) + \sum_{j \neq n} c_{nj} \varphi_j^{(0)}(1) \qquad \text{on } S_1 \tag{17.21}$$

$$\varphi_n(2) = \varphi_n^{(0)}(2) + \sum_{k \neq n} c_{nk} \varphi_k^{(0)}(2) \qquad \text{on } S_2, \tag{17.22}$$

where $\varphi_n^{(0)}$s are the eigenfunctions of the single-sphere problem. The eigenfunction $\varphi_k^{(0)}(2)$ as a double layer density generates a velocity field "$\boldsymbol{v}_k$" outside sphere 2. The inner product between this velocity field and the basis elements on the surface of sphere 1 is an important quantity. We introduce the notation,

$$\langle\, \varphi_j^{(0)}(1), \mathcal{K}\varphi_k^{(0)}(2)\,\rangle_1 = \int_{S_1} \varphi_j^{(0)}(1) \cdot \boldsymbol{v}_k \, dS \,, \tag{17.23}$$

so that *on* S_1

$$\int_{S_2} \boldsymbol{K}(\boldsymbol{x}, \boldsymbol{\xi}_2) \cdot \varphi_k^{(0)}(\boldsymbol{\xi}_2) \, dS_2 = \sum_j \varphi_j^{(0)}(1) \left\langle \varphi_j^{(0)}(1), \mathcal{K}\varphi_k^{(0)}(2) \right\rangle_1 . \tag{17.24}$$

On the surface of sphere 1, the eigenvalue problem, $\mathcal{K}(\varphi_n) = \lambda_n \varphi_n$ becomes

$$\begin{aligned} &\lambda_n^{(0)} \varphi_n^{(0)} + \sum_{j \neq n} c_{nj} \lambda_j^{(0)} \varphi_j^{(0)}(1) \pm \sum_j \left\langle \varphi_j^{(0)}(1), \mathcal{K}\varphi_k^{(0)}(2) \right\rangle_1 \varphi_j^{(0)}(1) \\ &= \lambda_n \varphi_n^{(0)} + \lambda_n \sum_{j \neq n} c_{nj} \varphi_j^{(0)}(1) \,. \end{aligned} \tag{17.25}$$

The first and second terms on the left-hand side of this equation result from the fact that the $\varphi_j^{(0)}$s are eigenfunctions of $\mathcal{K}$ restricted to S_1, with eigenvalues $\lambda_j^{(0)}$. Looking at each mode, we find the following set of equations:

$$\text{For } j = n: \quad \lambda_n = \lambda_n^{(0)} \pm \left\langle \varphi_j^{(0)}(1), \mathcal{K}\varphi_k^{(0)}(2) \right\rangle_1 \tag{17.26}$$

$$\text{For } j \neq n: \quad c_j = \frac{\pm \left\langle \varphi_j^{(0)}(1), \mathcal{K}\varphi_k^{(0)}(2) \right\rangle_1}{\lambda_n^{(0)} - \lambda_j^{(0)} \pm \left\langle \varphi_j^{(0)}(1), \mathcal{K}\varphi_k^{(0)}(2) \right\rangle_1} \,. \tag{17.27}$$

Here, $\pm$ denotes the sign used to construct the base solution, $\varphi_n^{(0)}(1) \pm \varphi_n^{(0)}(2)$.

We have arrived at the desired result. The eigenvalues of the two-sphere system are given by those of the single-sphere problem, plus a small perturbation proportional to the interaction factor, $\left\langle \varphi_j^{(0)}(1), \mathcal{K}\varphi_k^{(0)}(2) \right\rangle_1$, which we evaluate presently with an addition theorem. But first, we may estimate the R-dependence of the spectral radius with this limited information. From the discussion for the single sphere, we know that the dominant eigenfunctions (the ones with eigenvalue $-3/5$) generate Stokes quadrupole fields, which decay as

$|\boldsymbol{x} - \boldsymbol{x}_2|^{-3}$. The fact that $j = n$ determines the eigenvalue shift implies that we need the quadrupole moment induced on sphere 1, which from the Faxén relation is proportional to the *second* derivative of the incident field. Therefore, we expect the shift in the spectral radius to scale as $|\boldsymbol{x}_1 - \boldsymbol{x}_2|^{-5}$, which we now verify *via* the exact formula.

We require the following addition theorem for Stokes flow [35, 63]:

$$\begin{aligned}\left\langle \boldsymbol{\varphi}^{(3)}_{n'm'}(1), \mathcal{K}\boldsymbol{\varphi}^{(3)}_{nm}(2)\right\rangle &= (1+\lambda^{(0)}_{n'})(-1)^{m+n}\delta_{mm'}\sqrt{n(n+1)n'(n'+1)} \\ &\quad \times \frac{\eta_{nm}}{\eta_{n'm}} \begin{pmatrix} n+n' \\ n+m \end{pmatrix} \frac{-R^{-(n+n'+1)}}{(n+1)(n'+1)} \, .\end{aligned}$$

The factor of $(1+\lambda^{(0)}_{n'})$ takes into account the jump between the surface density $\boldsymbol{\varphi}(\boldsymbol{\xi}_2)$ on S_2 and the associated velocity field emanating from sphere 2. *This factor also ensures that the eigenvalues at* -1 *do not get shifted,* which we know has to be the case, since the eigenvalues corresponding to the null densities are always equal to -1, independent of the (multiparticle) geometry.

We now apply these results with the eigenvalue as $-3/(2n+1)$. The perturbation result for the two-sphere system becomes

$$\begin{aligned}\lambda_{2m} &= -\frac{3}{5} \pm \frac{2}{5}\left\langle \boldsymbol{\varphi}^{(3)}_{2m}(1), \mathcal{K}\boldsymbol{\varphi}^{(3)}_{2m}(2)\right\rangle \\ &= -\frac{3}{5} \pm (-1)^{m+1}\frac{4}{15}\begin{pmatrix} 4 \\ 2+m \end{pmatrix} R^{-5} \\ &= -\frac{3}{5} \pm \frac{(-1)^{m+1}32R^{-5}}{5(m+2)!\,(2-m)!}\end{aligned}$$

We may write these results explicitly as

$$\begin{aligned} m = 0: \quad \lambda &= -\frac{3}{5}\left[1 \pm \frac{8}{3}R^{-5}\right] \\ |m| = 1: \quad \lambda &= -\frac{3}{5}\left[1 \pm \frac{-16}{9}R^{-5}\right] \\ |m| = 2: \quad \lambda &= -\frac{3}{5}\left[1 \pm \frac{4}{9}R^{-5}\right] \, . \end{aligned}$$

There are five pairs, but two of these pairs are degenerate, so that there are three *distinct pairs*, with each pair consisting of a "bonding" and "anti-bonding" split. As with molecular orbitals, the value of m determines whether the "+" or "-" shifts the eigenvalue downwards.

In summary, the ten degenerate eigenvalues at $-3/5$ of the decoupled system splits into a set of six distinct eigenvalues with multiplicities: 1,2,2,2,2, and 1. The magnitude of the splits, as computed numerically and analytically, are in excellent agreement, as shown in Figure 17.4. (We defer until Chapter 19 the discussion on the discretization schemes for the numerical solution.) More importantly, in contrast with the more familiar situation in quantum mechanics, the shift in the spectrum as a result of hydrodynamic interactions is actually

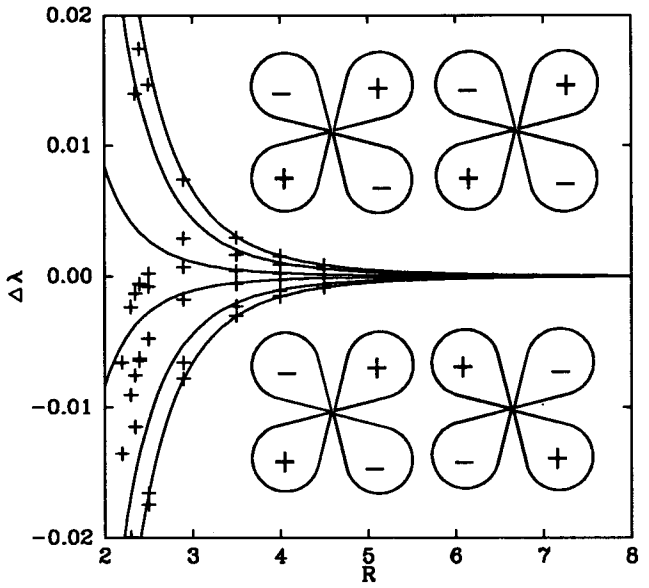

Figure 17.4: Comparison of numerical and asymptotic results for λ.

quite small. This has important ramifications for computations. We show in the following sections a deflate-and-iterate solution scheme, which consists of a deflation procedure for removing all eigenvalues at ± 1, and an iterative solution of the resulting set of equations. The iterations converge since the spectral radius of the deflated system is less than one. But now we know that the number of iterations is essentially the same as in the single-particle problem. For the sphere, according to the discussion above, the spectral radius for the two-sphere system remains approximately 0.6 (the single-sphere result) at all configurations except almost-touching spheres. We will in fact observe this property directly in multisphere problems, where we discover that the iterative solutions converge with essentially the same number of iterations as in the single-sphere problem.

17.3 Wielandt's Deflation

Consider the double layer IE of the second kind without any completion. We know now that the integral operator ("iteration operator" for direct iteration) there has spectral radius exactly one. Thus direct iteration would not be successful here, as spectral radius strictly less than one is required. However, if we can remove the endpoints of the spectrum, for example, by moving those eigenvalues to zero, *without affecting the rest of the eigenvalues*, the new modified spectrum will allow direct iterative solution. Such a modification is possible

by using *Wielandt's deflation.* (For a compact operator eigenvalues other than zero are isolated and removing the extreme eigenvalues will strictly diminish the spectral radius — if, to the contrary, the extreme eigenvalues were possibly accumulation points, there still could remain eigenvalues arbitrarily close to these, and the spectral radius would have to be defined as the *supremum* of the magnitudes of the eigenvalues, possibly not attained.)

Consider the Jordan form of a matrix. If the matrix happens to be diagonalizable, having only eigenvectors and no other principal vectors, the Jordan form is just the diagonal form of the matrix. Otherwise to each nontrivial Jordan chain there corresponds a Jordan block, in which the diagonal elements coincide with the eigenvalue in question and the upper bidiagonal is filled with ones. (Equivalently the lower bidiagonal could be used for the Jordan blocks; this corresponds to reversal of the order of the principal vectors in the basis used). So the Jordan form is just an "almost diagonal representation" of the original matrix, obtained by using the principal vectors as the basis for the vector space. This similarity transformation can be represented as $\boldsymbol{K} = \boldsymbol{B}\boldsymbol{J}\boldsymbol{B}^{-1}$, where $\boldsymbol{K}$ is the original matrix, $\boldsymbol{B}$ contains the principal vectors as its columns, and $\boldsymbol{J}$ is the Jordan form. On taking the adjoint of this equation the order of matrix multiplications is reversed, and we find $\boldsymbol{K}^* = \boldsymbol{B}^{-*}\boldsymbol{J}^*\boldsymbol{B}^*$; recall that for matrices the adjoint is the complex conjugated transpose. By inspection, $\boldsymbol{B}^{-*}$ must have the principal vectors of the adjoint as its columns. As $\boldsymbol{B}$ is obtained from the principal vectors of the original matrix, this shows that the two sets of principal vectors are *biorthogonal* bases for the vector space, meaning that the (complex) inner product of a fixed principal vector is zero with all but one of the adjoint's principal vectors.

Let $\boldsymbol{x}_i$ be the principal vectors of $\boldsymbol{K}$, and $\boldsymbol{y}_i$ be those of the adjoint $\boldsymbol{K}^*$. Represent the operator $\boldsymbol{x}_{\tilde{i}}\langle\cdot, \boldsymbol{y}_{\tilde{i}}\rangle$ (*no summation over* $\tilde{i}$) as a matrix relative to the basis given by the $\boldsymbol{x}_i$s. Due to the biorthogonality we have $\langle \boldsymbol{x}_j, \boldsymbol{y}_{\tilde{i}}\rangle = \langle \boldsymbol{x}_{\tilde{i}}, \boldsymbol{y}_{\tilde{i}}\rangle \delta_{\tilde{i}j}$, so that only elements in the $\tilde{i}$-column are nonzero. Moreover, this operator gives only multiples of $\boldsymbol{x}_{\tilde{i}}$, so that in that column only the $\tilde{i}$-element is nonzero. Thus in fact this operator is represented by the $\tilde{i}$-th diagonal element being $\langle \boldsymbol{x}_{\tilde{i}}, \boldsymbol{y}_{\tilde{i}}\rangle$ with all other elements being zeroes. Addition of this operator to the original operator $\boldsymbol{K}$ will correspond to modifying just one of the diagonal elements in the Jordan form; the result is not necessarily a Jordan form any more (namely, if $\boldsymbol{x}_{\tilde{i}}$ is a principal vector in a nontrivial Jordan chain), but, as it is still triangular, all the eigenvalues are visible on the diagonal. Therefore one of the eigenvalues has been modified (if the corresponding Jordan block was nontrivial the original eigenvalue has not been removed completely, just its multiplicity has changed), while the rest of these remain unchanged. Operators of the type above, here used for modifying the original matrix, are sometimes called *rank-one* operators or *tensor products.*

Let us now concentrate on eigenvectors, as a special case of principal vectors. The procedure above can be used when both an eigenvector of the original operator and the corresponding eigenvector of the adjoint are known. We can, however, get essentially the same effect with less information; this leads to actual

Wielandt's deflations. Consider first the case where only $\boldsymbol{x}_i^{\sim}$ is known. Instead of $\boldsymbol{y}_i^{\sim}$ we use just some vector $\boldsymbol{y}$ within the inner product part of the rank-one operator. When represented in the basis of principal vectors of the operator of interest $\boldsymbol{K}$, this corresponds to one nonzero row. By choosing $\boldsymbol{x}_i^{\sim}$ to be the first vector in the basis, this is the first row, and therefore addition to the original matrix $\boldsymbol{K}$ modifies its Jordan form again to a triangular form. This modification only changes one of the diagonal elements, therefore retaining the rest of the eigenvalues unchanged. The first diagonal element has been changed by adding the number $\langle \boldsymbol{x}_i^{\sim}, \boldsymbol{y} \rangle$ to it; this shows explicitly the change in that eigenvalue. Note that the order in which $\boldsymbol{x}_i^{\sim}$ and $\boldsymbol{y}$ are used in the tensor product is crucial: Switching them gives a rank-one operator without the desired properties in general. For the second case assume that $\boldsymbol{y}_i^{\sim}$ is known, while $\boldsymbol{x}_i^{\sim}$ is not. In place of $\boldsymbol{x}_i^{\sim}$ use some vector $\boldsymbol{x}$ to get the rank-one operator $\boldsymbol{x}\langle \cdot, \boldsymbol{y}_i^{\sim} \rangle$. This, when represented in the same basis as the original Jordan form, gives just one nonzero column. By rearranging the basis as necessary, this column can be chosen to be the last. Again, addition of such a tensor product keeps the original Jordan form triangular, and the eigenvalues remain unchanged, except for the last one. The shift in the last eigenvalue is explicitly given by $\langle \boldsymbol{x}, \boldsymbol{y}_i^{\sim} \rangle$.

In summary, Wielandt's deflation can be carried out when either an eigenvector of the operator itself or that of its adjoint is known. The former must be used outside the inner product in the rank-one modification, and the latter inside the inner product. The rank-one modification will modify only the eigenvalue corresponding to the eigenvector used, leaving the rest unchanged. If the eigenvector used corresponds to a trivial Jordan block, no new eigenvectors with the relevant eigenvalue are created; otherwise, the situation gets more complicated, but the Jordan form still provides some insight as to what happens.

Now we consider multiple Wielandt's deflations done at once. Suppose we know two eigenvectors $\boldsymbol{x}_1$ and $\boldsymbol{x}_2$ of $\boldsymbol{K}$. In the basis used for the Jordan canonical form of $\boldsymbol{K}$, the operators $\boldsymbol{x}_1\langle \cdot, \boldsymbol{z}_1 \rangle$ and $\boldsymbol{x}_2\langle \cdot, \boldsymbol{z}_2 \rangle$ are represented each by a single nonzero row. Here the $\boldsymbol{z}$-vectors are arbitrary to start with. Addition of both these operators to $\boldsymbol{K}$ will modify just two rows in the original Jordan form, and by permutation of the basis used these can be chosen as the first two rows. Now the resulting matrix is *block-triangular*, with the lower left-hand side $(n-2) \times 2$ block being zero, and the diagonal blocks being square. For this situation it is known from linear algebra (theory of determinants) that the eigenvalues of the total matrix are given by those of the diagonal blocks. The latter of these diagonal blocks is again triangular, unchanged from the original Jordan form, and therefore the corresponding eigenvalues visible on the diagonal have remained unchanged, as with simple deflation. The modification to the first 2×2 diagonal block is given by the matrix

$$\begin{bmatrix} \langle \boldsymbol{x}_1, \boldsymbol{z}_1 \rangle & \langle \boldsymbol{x}_2, \boldsymbol{z}_1 \rangle \\ \langle \boldsymbol{x}_1, \boldsymbol{z}_2 \rangle & \langle \boldsymbol{x}_2, \boldsymbol{z}_2 \rangle \end{bmatrix}, \tag{17.28}$$

and in general it would be difficult to give a *nice* formula for the change in the original eigenvalues due to this modification. The situation is considerably

simplified by requiring that the off-diagonal elements in this 2×2 matrix are zeroes, while the diagonal elements are not; such orthogonality requirements are easy to accommodate in practice. If the 2×2 matrix above is invertible, there exist linear combinations of the z-vectors such that when used in place of these the 2×2 identity matrix results. This procedure can be applied to as many vectors as is necessary, before carrying out the deflation; here two vectors were used just to keep the notation simple and easy to follow.

17.4 Deflation for a Single Particle

From Theorem 1 it is known that -1 is an eigenvalue of $\mathcal{K}$, corresponding to six linearly independent eigenfunctions that are given by rigid-body motions. In addition, the corresponding Jordan blocks are trivial, so that deflation with these eigenfunctions really removes the eigenvalue -1 completely; recall that in the case of nontrivial Jordan blocks the same eigenvalue would remain on the diagonal of the original Jordan form after deflation using only the eigenvectors.

The original operator in the unmodified double layer equation is $1 + \mathcal{K}$. On deflation using the known RBM null functions, we need to add six rank-one modifications, namely,

$$\sum_{i=1}^{3} \{U_i \langle \varphi, z_i \rangle + (\omega_i \times r) \langle \varphi, Z_i \rangle\} , \tag{17.29}$$

where the functions z_i and Z_i are suitably chosen. Note that the known eigenfunctions of the operator are used for output, not within the inner product, as Wielandt's deflation requires. Furthermore, it seems to be easiest to choose the set of U_is and $\omega_i \times r$s to form an orthonormal set with respect to the natural inner product, and further choose the z_is and Z_is to equal these functions, respectively. This can be accomplished by using the Gram–Schmidt orthonormalization procedure (normalizing to unit length after the orthogonalization) to some translations and rotations, and ensures the orthonormality of the functions used within the inner products, which is useful on doing controlled multiple deflation. Since all the eigenvectors correspond to the same eigenvalue, the orthogonalization forming linear combinations again gives eigenvectors.

Thus the added part now looks like

$$\sum_{i=1}^{3} \{U_i \langle \varphi, U_i \rangle + (\omega_i \times r) \langle \varphi, (\omega_i \times r) \rangle\}. \tag{17.30}$$

It is easy to see that translations in dot-product orthogonal directions are mutually orthogonal also with respect to the natural inner product over the boundary surface, and the rotational eigenfunctions are orthogonal to these iff the origin (center of rotation) is chosen to be the center of mass of the boundary:

$$\oint_S r \, dS = 0 . \tag{17.31}$$

Then on orthonormalization the first rotational eigenfunction is just normalized and therefore it remains a rotation, while the second and third of these get rotational additions only, since they already are orthogonal to translational eigenfunctions. Therefore orthogonalization just modifies the rotational velocities ω_i. For example, for a sphere it is easy to verify directly that the ω_is can be chosen in the directions of the coordinate axes, but in general this need not be the case.

Typically the Gram–Schmidt procedure will give axes of rotation that are *not* orthogonal with respect to the *dot product.* Another way to perform the orthogonalization is to choose the orthogonal coordinate axes so that the moment of inertia tensor, for the surface with uniform mass-density, is diagonalized, keeping the origin at the center of mass. In practice this only requires diagonalizing a 3×3 symmetric matrix, and is easily incorporated into the numerical codes. The major advantage of the latter procedure is keeping the rotation axes mutually orthogonal, and these axes can be chosen to be the coordinate axes. This simplifies the writing of codes to some extent (see Chapter 19). Also we see that for most particle shapes (*i.e.*, those whose moment of inertia tensor has three distinct eigenvalues) there will be a unique coordinate system, determined by the geometry, that automatically orthogonalizes the "natural basis" for RBMs. An important point raised in Chapter 5 should be re-emphasized here: *This natural choice of the origin and coordinate axes, as motivated by computational efficiency, differs from that dictated by classical hydrodynamics (diagonalization of the resistance/mobility tensors).* In general, one should not expect superior computational techniques to result from the use of physical insight alone, and it is precisely in these instances that mathematical analysis plays an important role.

Now the rank-one operators in the sum above each modify one row of the original Jordan form, the diagonal modification being $+1$, with other elements being zero in the corresponding diagonal block. This modification shifts the original eigenvalue -1 of $\mathcal{K}$ to 0.

The modification above resembles that used by Power and Miranda. The main difference is that instead of using total forces and torques on adding the missing part of the range, one now uses translation and rotation velocities. These are naturally connected with the total forces and torques in a linear fashion, through either the resistance or the mobility matrix. In any case a deduction similar to that used on explaining the bordering method shows that the range completion is carried out by the deflation above. Therefore two things have been accomplished at once here: the shift of one endpoint of the spectrum, and range completion of the double layer operator.

It is noteworthy that, although traditionally resistance problems have been favored over mobility problems, Wielandt's deflation here is only possible for problems of the latter kind. The reason for the traditional trend has been that for mobility problems the given data (total forces and torques) do not supply boundary conditions for use with ordinary methods of solving partial differential equations. For integral equation formulations the situation is different, as was

already seen when the canonical equations were presented.

One of the endpoints of the spectrum of $\mathcal{K}$ still remains, namely, that at 1. In order to make the direct (Picard) iteration possible, also this has to be moved towards the origin. Whether a single surface is considered a particle or a container affects only the direction of the surface normal in the definition of the integral operator $\mathcal{K}$; this change corresponds to multiplication of the operator with -1. Thus for "particle-$\mathcal{K}$" the eigenvalue 1 corresponds to -1 for a "container-$\mathcal{K}$," and the eigenfunction is the container null function of Theorem 2. This eigenfunction is not available for a general surface shape, but the adjoint eigenfunction is. According to Theorem 2 the adjoint eigenfunction is the surface normal, and the corresponding Jordan block is again trivial. In Wielandt's deflation the adjoint eigenfunction is used within the inner product, and the addition must be of the form

$$z\langle\varphi,\hat{n}\rangle\ , \tag{17.32}$$

where z is a suitable vector not orthogonal to $\hat{n}$. This condition is most certainly satisfied by the choice $z = a\hat{n}$ with $a \neq 0$ a constant. It seems optimal for the convergence rate of the iterations to shift the original eigenvalue 1 of $\mathcal{K}$ to 0, and the shift caused by addition of the rank-one operator above is $a\langle\hat{n},\hat{n}\rangle = a|S|$, where $|S|$ denotes the surface area. Thus the proper choice is $a = -1/|S|$. Please note that although $\hat{n}$ is a unit vector in the norm induced by the ordinary dot product for vectors, the same clearly need not hold with respect to the natural inner product on the surface S.

The effect of this deflation differs somewhat from the previous ones, as this is not related to range completion. The role of this latter deflation is purely mathematical, making direct iteration possible. Thus the effect of the deflation, *i.e.*, changing the original operator, has to be compensated for. Luckily this is also easy to accomplish. First note that here the adjoint eigenvector satisfies the relation $\mathcal{K}^*\hat{n} = \hat{n}$. Denote by $\mathcal{H}$ the operator resulting from the previous multiple deflations using the RBM null functions of $(1 + \mathcal{K})$. Then $(1 + \mathcal{H})$ is invertible and $(1 + \mathcal{H})^*\hat{n} = 2\hat{n}$. Therefore we first take the adjoint of the deflated operator

$$(1 + \mathcal{H} + a\hat{n}\langle\cdot,\hat{n}\rangle)^* = 1 + \mathcal{H}^* + a^*\hat{n}\langle\cdot,\hat{n}\rangle)\ . \tag{17.33}$$

(In general, on taking the adjoint the two vectors defining a tensor product are switched, while scalars are complex-conjugated.) On multiplying from left with $(1 + \mathcal{H}^*)^{-1}$ we find

$$(1 + \mathcal{H}^*)^{-1}(1 + \mathcal{H} + a\hat{n}\langle\cdot,\hat{n}\rangle)^* = 1 + (a^*\hat{n}/2)\langle\cdot,\hat{n}\rangle\ . \tag{17.34}$$

Taking the adjoint of this equation reveals that

$$(1 + \mathcal{H} + a\hat{n}\langle\cdot,\hat{n}\rangle)(1 + \mathcal{H})^{-1} = 1 + (a\hat{n}/2)\langle\cdot,\hat{n}\rangle \tag{17.35}$$

or

$$(1 + \mathcal{H})^{-1} = (1 + \mathcal{H} + a\hat{n}\langle\cdot,\hat{n}\rangle)^{-1}(1 + (a\hat{n}/2)\langle\cdot,\hat{n}\rangle)\ . \tag{17.36}$$

Therefore, instead of solving $(1+\mathcal{H})\boldsymbol{x}=\boldsymbol{b}$ for $\boldsymbol{x}$, we can equivalently solve

$$(1+\mathcal{H}+a\hat{\boldsymbol{n}}\langle\cdot,\hat{\boldsymbol{n}}\rangle)\,\boldsymbol{x}=(1+(a\hat{\boldsymbol{n}}/2)\langle\cdot,\hat{\boldsymbol{n}}\rangle)\boldsymbol{b}\;. \tag{17.37}$$

Thus all that is needed is a simple premultiplication of the data vector, giving $\tilde{\boldsymbol{b}}$, before the iterative solution $\boldsymbol{x}_{i+1}=-\mathcal{H}\boldsymbol{x}_i-a\hat{\boldsymbol{n}}\langle\boldsymbol{x}_i,\hat{\boldsymbol{n}}\rangle+\tilde{\boldsymbol{b}}$ is carried out.

17.5 Deflation for a Container

Handling of the container problem is similar in most essential features to that of the handling of a single particle. The major difference is that now the deficiency in the range is only of dimension one, while at the other endpoint of the spectrum a sixfold deflation is needed with compensation. This is just because on switching from a particle to a container the operator has experienced a sign change, and the roles of the endpoints of the spectrum have been reversed.

The container null function is not known in general, but the adjoint null function is again the surface normal. Thus the natural deflation is of the form

$$a\hat{\boldsymbol{n}}\langle\cdot,\hat{\boldsymbol{n}}\rangle\;, \tag{17.38}$$

where $\hat{\boldsymbol{n}}$ is as usual the unit surface normal, and a is a scalar that normalizes this rank-one modification. As in the previous section, the choice $a=1/|S|$, where $|S|$ is the surface area, shifts the eigenvalue to 0. Recall that this normalization comes from using the natural inner product over the surface. Mathematically this deflation obviously works; physically the addition is in the direction of $\hat{\boldsymbol{n}}$, and this is because we need a non-mass-conserving addition to the double layer representation on dealing with a bounded volume to be able to comply to arbitrary (possibly non-mass-conserving) data.

Now the range completion is done, and the other endpoint of the spectrum, namely 1, is dealt with. At this endpoint the eigenfunctions are the rigid-body motions, the dimension of the eigenspace being six and the corresponding Jordan blocks trivial. Therefore there are no serious mathematical difficulties in carrying out the deflations. Let $\boldsymbol{\varphi}_i$, $i=1,\ldots,6$, be the RBM eigenfunctions, *orthonormal* with respect to the natural inner product. Then the modification necessary is

$$\boldsymbol{M}=-\sum_{i=1}^{6}\boldsymbol{\varphi}_i\langle\cdot,\boldsymbol{\varphi}_i\rangle\;, \tag{17.39}$$

where the minus sign is necessary, since this time we are shifting eigenvalues that were originally 1 to 0. Denote again the operator after the previous (range completing) deflation by $\mathcal{H}=\mathcal{K}+a\hat{\boldsymbol{n}}\langle\cdot,\hat{\boldsymbol{n}}\rangle$. Then $(1+\mathcal{H})$ is invertible, and $(1+\mathcal{H})^{-1}\boldsymbol{\varphi}_i=(1/2)\boldsymbol{\varphi}_i$ for the RBM eigenfunctions. From this it easily follows that

$$(1+\mathcal{H})^{-1}=(1+(1/2)\boldsymbol{M})\,(1+\mathcal{H}+\boldsymbol{M})^{-1}\;. \tag{17.40}$$

This means that, for a container, we should first iteratively solve the equation

$$(1+\mathcal{H}+\boldsymbol{M})\,\boldsymbol{x}=\boldsymbol{b} \tag{17.41}$$

for $\boldsymbol{x}$, this being done with the Picard iteration $\boldsymbol{x}_{i+1} = -(\mathcal{H} + \boldsymbol{M})\,\boldsymbol{x}_i + \boldsymbol{b}$, and then premultiply the intermediate result $\boldsymbol{x}$ to get *the final result* $(1 + (1/2)\boldsymbol{M})\,\boldsymbol{x}$. Note the difference with the case of a particle, where the data were premultiplied before the iterations, and these directly gave the final result.

17.6 Multiparticle Problems in Bounded and Unbounded Domains

The deflations for a particle and a container surface have been discussed at length in the previous two sections. In this section we indicate how to deal with more complex cases, involving multiple particles and possibly also a container. The case of multiple containers is not of practical interest; we only deal with connected fluid domains, and these have at most one container boundary. The development of the theory here will utilize orthogonal projections, and the previous cases with a single boundary could have been handled similarly, as they are only special cases. We hope that the previous approaches complement the one given here, making it easier to follow the presentation.

Let S_i, $i = 1, \ldots, N$, be disjoint particle surfaces and S_c a surrounding container surface. The totality of surfaces is denoted by S. First we carry out the "physical deflations" necessary for range completion and removal of indeterminacies in the double layer density. Then the "mathematical deflations" are discussed at length. The purpose of the latter deflations is again to make the spectrum of the "iteration operator" in the second-kind equation small enough, *i.e.*, such that all its eigenvalues are strictly less than one in magnitude, and this mathematical trick needs to be compensated for in the solution procedure, while the physical deflations need no compensation. For analytical purposes the physical deflations would suffice, and the shift of the other endpoint of the spectrum serves only numerical purposes.

Let φ_{ij} be the "j-th RBM of particle i" ($j = 1, \ldots, 6$); each of these double layer densities attains nonzero values only on one particle surface S_i and $\mathcal{K}\varphi_{ij} = -\varphi_{ij}$. Assume these densities are orthonormal

$$\langle \varphi_{ij}, \varphi_{kl} \rangle = \delta_{ik}\delta_{jl}. \tag{17.42}$$

Here the δ_{ik} -part is trivially satisfied, and in practice the Gram–Schmidt orthonormalization needs to be applied separately for each i over the indices $j = 4, 5, 6$ if for each particle surface its center of mass is used as the center of rotations. These are $6N$ of the $6N + 1$ linearly independent eigenvectors with eigenvalue -1. Again the remaining container null function is not explicitly known in general, but instead the adjoint eigenfunction $\psi_t = -\mathcal{K}^*\psi_t$ is known to be

$$\psi_t = \alpha_t \hat{\boldsymbol{n}}, \tag{17.43}$$

where $\hat{\boldsymbol{n}}$ is the unit normal pointing into the fluid on all of S and the normalization is $\alpha_t = |S|^{-1/2}$. Now it is natural to carry out the Wielandt's deflations

and define

$$\mathcal{H} = \mathcal{K} + \varphi_{ij}\langle \cdot, \varphi_{ij}\rangle + \psi_t\langle \cdot, \psi_t\rangle \ , \tag{17.44}$$

where *the summation convention was used, as is frequently done in the rest of this section.*

Now the physical deflations have been carried out and $(1+\mathcal{H})$ is invertible, as the eigenvalues at -1 of $\mathcal{K}$ have been shifted to 0 for $\mathcal{H}$. Otherwise the spectra of $\mathcal{H}$ and $\mathcal{K}$ coincide. For any smooth surface field $\boldsymbol{u}$ (velocity BCs) there exists a unique φ such that

$$(1+\mathcal{H})\varphi = \boldsymbol{u} \ . \tag{17.45}$$

Let us now interpret the definition of $\mathcal{H}$ physically. Any nonzero RBMs of the particles (except when the same RBM prevails on all the particles *and* on the container) would necessarily correspond to some nonzero forces or torques acting on them, and are thus not represented by a double layer alone. These particle RBMs are added separately. The additions so far are mass conserving, and only BCs, similarly mass conserving, could be satisfied without the final addition (deflation with ψ_t), which removes this restriction.

Consider now a mobility problem, with given forces $\boldsymbol{F}_i$ and torques $\boldsymbol{T}_i$ acting at points $\boldsymbol{x}_i$ within each particle. Define

$$\boldsymbol{u} = \boldsymbol{F}_i \cdot \mathcal{G}(\boldsymbol{x}-\boldsymbol{x}_i)/(8\pi\mu) - \frac{1}{2}(\boldsymbol{T}_i \times \nabla)\cdot \mathcal{G}(\boldsymbol{x}-\boldsymbol{x}_i)/(8\pi\mu) \ . \tag{17.46}$$

Using these BCs we solve φ from $(1+\mathcal{H})\varphi = \boldsymbol{u}$. The non-mass-conserving term in $\mathcal{H}$ must vanish, as it is the only such term in the whole equation: $\langle \varphi, \psi_t\rangle = 0$. The remaining equation is rewritten as

$$\varphi_{ij}\langle \varphi, \varphi_{ij}\rangle = -(1+\mathcal{K})\varphi + \boldsymbol{u}. \tag{17.47}$$

The first term on the RHS here gives no total force or torque, and so the RBMs on the LHS must correspond to the forces and torques used on forming $\boldsymbol{u}$. Thus the mobility problem can be directly solved.

The spectrum of $\mathcal{H}$ now lies in the real interval $(-1,1]$, and in order to enable iterative solution, deflations are needed so that the modified spectrum is within $(-1,1)$. For both $\mathcal{K}$ and $\mathcal{H}$ the multiplicity of the eigenvalue 1 is $6+N$. Explicitly six linearly independent eigenfunctions are given by the RBMs on the totality of surfaces S, for which

$$\mathcal{K}\varphi_{tj} = \varphi_{tj}, \text{ for } j = 1,\ldots,6 \tag{17.48}$$

(by invoking Gram–Schmidt, if necessary, these are assumed orthonormal with respect to the natural inner product), and N orthonormal adjoint eigenfunctions are given by the scaled particle surface normals

$$\psi_i = \mathcal{K}^*\psi_i = \begin{cases} \alpha_i \hat{\boldsymbol{n}} & \text{on } S_i \\ 0 & \text{otherwise.} \end{cases} \tag{17.49}$$

For normalization choose $\alpha_i = |S_i|^{-1/2}$. These were orthonormalized eigenfunctions of $\mathcal{K}$ and its adjoint, and while for $\mathcal{H}$ and its adjoint each eigenvalue and its multiplicity are the same as for $\mathcal{K}$, the corresponding eigenfunctions are different.

So far everything here has been very similar to the cases with single connected boundaries, *i.e.*, a single particle or a container. It is here in the mathematical deflations that complications arise, as these need to be done and compensated for simultaneously both for eigenfunctions and adjoint eigenfunctions when particles and a container coexist. Suppose we have orthonormal sets of eigenfunctions of $\mathcal{H}$ and its adjoint, such that

$$\mathcal{H}\varphi'_j = \varphi'_j, \text{ for } j = 1, \ldots, 6 \tag{17.50}$$

$$\mathcal{H}^*\psi'_i = \psi'_i, \text{ for } i = 1, \ldots, N. \tag{17.51}$$

Define the "left" projection

$$\mathcal{P}_L = \psi'_i\langle \cdot, \psi'_i\rangle \tag{17.52}$$

and the "right" projection

$$\mathcal{P}_R = \varphi'_j\langle \cdot, \varphi'_j\rangle \ ; \tag{17.53}$$

the motivation for the names will be apparent presently.

Immediately one can verify that

$$\mathcal{H}\mathcal{P}_R = \mathcal{P}_R \tag{17.54}$$

$$\mathcal{H}^*\mathcal{P}_L = \mathcal{P}_L \ , \tag{17.55}$$

and taking the adjoint of the latter equation gives

$$\mathcal{P}_L\mathcal{H} = \mathcal{P}_L. \tag{17.56}$$

Recall that for projections $\mathcal{P}$ in general, $\mathcal{P} = \mathcal{P}^* = \mathcal{P}^2$. Note also that due to mutual orthogonality

$$\mathcal{P}_R\mathcal{P}_L = \mathcal{P}_L\mathcal{P}_R = 0. \tag{17.57}$$

Now the natural deflated operator is

$$\tilde{\mathcal{H}} = \mathcal{H} - \mathcal{P}_R - \mathcal{P}_L, \tag{17.58}$$

in which the eigenvalue 1 has been shifted to 0. Using the special properties of the projections when multiplied with $\mathcal{H}$, the following simple connection between $(1 + \mathcal{H})$ and $(1 + \tilde{\mathcal{H}})$ is found:

$$(1 - \mathcal{P}_L/2)(1 + \mathcal{H})(1 - \mathcal{P}_R/2) = 1 + \tilde{\mathcal{H}}. \tag{17.59}$$

Operators of the type $(1 - \mathcal{P}/2)$ are invertible, the inverse being $(1 + \mathcal{P})$, so that the relation above can easily be inverted.

The equation $(1 + \mathcal{H})\boldsymbol{\varphi} = \boldsymbol{u}$ is equivalent to

$$\tilde{u} = (1 - \mathcal{P}_L/2)\boldsymbol{u} \tag{17.60}$$

$$(1 + \tilde{\mathcal{H}})\tilde{\boldsymbol{\varphi}} = \tilde{u} \tag{17.61}$$

$$\boldsymbol{\varphi} = (1 - \mathcal{P}_R/2)\tilde{\boldsymbol{\varphi}}, \tag{17.62}$$

and this gives the steps for the computational procedure. First transform the data. Then solve the second-kind equation, which now allows direct iterative solution. Finally modify the found solution with a simple linear transformation.

In practice one should not form $\tilde{\mathcal{H}}$ explicitly at all, as this would be a computationally expensive matrix operation. Rather, always compute

$$(1+\tilde{\mathcal{H}})\tilde{\varphi} = (1+\mathcal{H}-\mathcal{P}_L-\mathcal{P}_R)\tilde{\varphi}, \tag{17.63}$$

where vectors are multiplied by matrices or other vectors on forming the projections. Similarly $\mathcal{H}$ should not be explicitly formed from $\mathcal{K}$, but rather have it "operationally defined" in a subroutine.

Now an algorithmic approach to finding the orthonormal eigenvectors φ_j' and ψ_i' will be given. First note that

$$(1+\mathcal{H})\varphi_{tj} = 2\varphi_{tj} + \varphi_{ik}\langle\varphi_{tj},\varphi_{ik}\rangle \tag{17.64}$$

and

$$(1+\mathcal{H})\varphi_{ik} = \varphi_{ik}. \tag{17.65}$$

Then for

$$\varphi_j'' = \varphi_{tj} + \varphi_{ik}\langle\varphi_{tj},\varphi_{ik}\rangle \tag{17.66}$$

we have

$$(1+\mathcal{H})\varphi_j'' = 2\varphi_j'' \,. \tag{17.67}$$

These found six eigenfunctions of $\mathcal{H}$ can numerically easily be orthonormalized with the Gram–Schmidt procedure to get the φ_j' vectors that define the projection $\mathcal{P}_R$ for numerical purposes. In fact

$$\varphi_{ik}\langle\varphi_{tj},\varphi_{ik}\rangle = \begin{cases} 0 & \text{on } S_c \\ \varphi_{tj} & \text{otherwise,} \end{cases} \tag{17.68}$$

and no cumbersome double sums need be evaluated. Thus

$$\varphi_j'' = \begin{cases} \varphi_{tj} & \text{on } S_c \\ 2\varphi_{tj} & \text{otherwise.} \end{cases} \tag{17.69}$$

Using the general identity $(a\langle\cdot,b\rangle)^* = b\langle\cdot,a\rangle$ it is easy to verify that

$$(1+\mathcal{H})^*\psi_i = 2\psi_i + \frac{\alpha_t}{\alpha_i}\psi_t, \tag{17.70}$$

and since $(1+\mathcal{H})^*\psi_t = \psi_t$ we have

$$(1+\mathcal{H})^*\psi_i'' = 2\psi_i'' \tag{17.71}$$

for

$$\psi_i'' = \psi_i + \frac{\alpha_t}{\alpha_i}\psi_t. \tag{17.72}$$

Without the use of Gram–Schmidt these found N eigenvectors are nonorthogonal. In fact,

$$\langle\psi_i'',\psi_j''\rangle = \delta_{ij} + 3\frac{\alpha_t^2}{\alpha_i\alpha_j}. \tag{17.73}$$

Using these known inner products one could choose to carry out the Gram–Schmidt procedure numerically. The form of the inner products here is, however, simple enough to allow doing the orthonormalization analytically, as will now be shown.

Define the column vector $\boldsymbol{y} \in R^N$ by $y_i = \alpha_i/\alpha_i$, and the matrix $\boldsymbol{A} = (a_{ij})_{N\times N}$ by $a_{ij} = \langle \boldsymbol{\psi}_i'', \boldsymbol{\psi}_j'' \rangle$. Then $\boldsymbol{A} = 1 + 3\boldsymbol{y}\boldsymbol{y}^t$. Let

$$\boldsymbol{\psi}_i' = b_{ij}\boldsymbol{\psi}_j'' \tag{17.74}$$

and require orthogonality

$$\langle \boldsymbol{\psi}_i', \boldsymbol{\psi}_j' \rangle = \delta_{ij}. \tag{17.75}$$

This requirement is equivalent to the matrix equation

$$\boldsymbol{B}\boldsymbol{A}\boldsymbol{B}^t = 1, \tag{17.76}$$

where $\boldsymbol{B} = (b_{ij})_{N\times N}$. Assume that we can find a solution of the form $\boldsymbol{B} = 1 + \beta\boldsymbol{y}\boldsymbol{y}^t = \boldsymbol{B}^t$. Then $\boldsymbol{B}$ and $\boldsymbol{A}$ commute, and we find

$$\boldsymbol{B} = \boldsymbol{A}^{-1/2}. \tag{17.77}$$

Let $\mathcal{P} = |\boldsymbol{y}|^{-2}\boldsymbol{y}\boldsymbol{y}^t$ be the orthogonal projection in the direction of $\boldsymbol{y}$. Write

$$\boldsymbol{A} = [1 - \mathcal{P}] + (3|\boldsymbol{y}|^2 + 1)\mathcal{P}, \tag{17.78}$$

which expresses $\boldsymbol{A}$ as the weighted sum of two mutually orthogonal projections. In this form functions of $\boldsymbol{A}$ can be formed analogously to corresponding operations on diagonal matrices. Thus

$$\boldsymbol{A}^{-1/2} = [1 - \mathcal{P}] + \mathcal{P}/\sqrt{3|\boldsymbol{y}|^2 + 1} = 1 + \left((3|\boldsymbol{y}|^2 + 1)^{-1/2} - 1\right)\frac{\boldsymbol{y}\boldsymbol{y}^t}{|\boldsymbol{y}|^2}. \tag{17.79}$$

Since $|S| = |S_c| + \sum_{i=1}^N |S_i|$,

$$|\boldsymbol{y}|^2 = \sum_{i=1}^N \frac{\alpha_i^2}{\alpha_i^2} = \left(\sum_{i=1}^N |S_i|\right)/|S| = 1 - |S_c|/|S|, \tag{17.80}$$

and computing $|\boldsymbol{y}|^2$ is easy.

We found that $\boldsymbol{B} = 1 + \beta\boldsymbol{y}\boldsymbol{y}^t$ with

$$\beta = |\boldsymbol{y}|^{-2}\left(\frac{1}{\sqrt{3|\boldsymbol{y}|^2 + 1}} - 1\right), \tag{17.81}$$

so that

$$\boldsymbol{\psi}_i' = b_{ij}\boldsymbol{\psi}_j'' = \boldsymbol{\psi}_i'' + \beta y_i(y_j\boldsymbol{\psi}_j''). \tag{17.82}$$

Numerically the orthonormalization is now in a very efficient form, as the sum $y_j\boldsymbol{\psi}_j''$ is calculated just once, and each $\boldsymbol{\psi}_i''$ is corrected with a multiple of this.

As a check let us inspect what happens when the container boundary becomes very large. Firstly, when $|S_c| \approx |S|$, $\frac{\alpha_t}{\alpha_i} \approx 0$ and $\psi_i'' \approx \psi_i$. Secondly $|y|^2 \approx 0$ implies $\beta|y|^2 \approx 0$, and thus $B \approx 1$. Then also $\psi_i' \approx \psi_i''$. Therefore $\psi_i' \approx \psi_i$, and the N orthonormal eigenfunctions of the adjoint — used for the mathematical deflations — are approximated quite closely by the N scaled particle surface normals. This is reasonable, since we expect the effect of the container surface to diminish as it "expands to infinity."

Also we note that if there is no container $\mathcal{P}_R = \mathbf{0}$, and the mathematical deflations assume the form found when a single particle was considered. Similarly for a container alone $\mathcal{P}_L = \mathbf{0}$, and the previously found result is recovered.

In summary this section has shown how the original double layer operator in discretized form can be so modified that efficient iterative solution of *mobility problems* is possible. Currently the authors are not aware of a deflation procedure that would enable similar modification of the second-kind integral equations for the iterative solution of resistance problems, except in special cases such as a spherical particle. Thus it seems that on using the second-kind IE formulations mobility problems will be favored over resistance problems, while the use of conventional solution methods leads to favoring resistance problems.

17.7 Iterative Solution of the Tractions for a Mobility Problem

Numerically the most important properties of the deflated double layer equations are the well-posedness and the feasibility of efficient iterative solutions. The latter especially is important since the linear systems are large and dense, and ordinary solution methods would be too expensive. Another useful feature of the iterative solution method is that good initial guesses can be utilized. An application where good initial guesses are available (except for the first time step) is the simulation of some system of particles over some period of time. With the quasi-steady approximation, at each time step one then solves the steady Stokes equations and uses the found RBM velocities to determine the particle configuration after a small increment in time, at which point a new steady Stokes solution is computed. When the changes of configuration are small, the previous solution provides a good approximation to the current one, and a small number of iterations will suffice.

In this section we show how the tractions can also be found iteratively for mobility problems. In fact we want the tractions that actually correspond to the given external forces and torques acting on the rigid particles, with as few calculations as possible, and not just tractions corresponding to some RBM. In some sense our mobility-based tractions complement Brenner's result relating the "resistance-based" tractions to mappings on total force and torque. The Lorentz reciprocal theorem can be used with the Riesz theorem (see below) to show that the "mobility-based" RBM tractions correspond to linear functionals that map a given surface velocity to components of that RBM that absorbs the

total forces and torques, leaving the rest of the disturbance field representable by a double layer alone. The same result can be reached, based on our knowledge about the double layer operator, without using the Lorentz reciprocal theorem; the linear algebra steps required will also be shown in the following paragraphs.

Let $\boldsymbol{u}$ be a given velocity surface field, $\boldsymbol{v}_{RBM}$, the velocity field corresponding to total force $\boldsymbol{F}$ and torque $\boldsymbol{T}$ (mobility solution), and $\boldsymbol{u}_{RBM} = \boldsymbol{U} + \boldsymbol{\omega} \times \boldsymbol{r}$ such RBM velocity that $\boldsymbol{u} - \boldsymbol{u}_{RBM}$ is force- and torque-free. We will use the fact that

$$\langle \boldsymbol{u}, \hat{\boldsymbol{n}} \cdot \boldsymbol{\sigma}(; \boldsymbol{v}_{RBM}) \rangle = -(\boldsymbol{U} \cdot \boldsymbol{F} + \boldsymbol{\omega} \cdot \boldsymbol{T}) \ . \tag{17.83}$$

(The Lorentz reciprocal theorem was implicitly used here.) This shows the physical significance of mobility-based tractions: They map a given velocity field, $\boldsymbol{u}$, to (components of) such an RBM that absorbs the total force and torque, as claimed above. To derive this, we reason as follows:

$$\begin{aligned} 0 &= \langle \hat{\boldsymbol{n}} \cdot \boldsymbol{\sigma}(; \boldsymbol{u} - \boldsymbol{u}_{RBM}), \boldsymbol{v}_{RBM} \rangle \\ &= -\langle \boldsymbol{u}_{RBM}, \hat{\boldsymbol{n}} \cdot \boldsymbol{\sigma}(; \boldsymbol{v}_{RBM}) \rangle + \langle \boldsymbol{u}, \hat{\boldsymbol{n}} \cdot \boldsymbol{\sigma}(; \boldsymbol{v}_{RBM}) \rangle \\ &= (\boldsymbol{U} \cdot \boldsymbol{F} + \boldsymbol{\omega} \cdot \boldsymbol{T}) + \langle \boldsymbol{u}, \hat{\boldsymbol{n}} \cdot \boldsymbol{\sigma}(; \boldsymbol{v}_{RBM}) \rangle \ . \end{aligned}$$

It may be helpful to see how this works out for a single sphere. According to the Faxén law (Chapter 3), a force-free sphere, subject to the surface field $\boldsymbol{u}$, must translate as

$$\boldsymbol{U} = (\boldsymbol{u} + \frac{a^2}{6} \nabla^2 \boldsymbol{u})|_{x=0} = \frac{1}{4\pi a^2} \oint_{S_p} \boldsymbol{u} \, dS \ , \tag{17.84}$$

so that

$$\boldsymbol{U} \cdot \boldsymbol{F} = \frac{1}{4\pi a^2} \oint_{S_p} \boldsymbol{u} \cdot \boldsymbol{F} \, dS = \frac{1}{4\pi a^2} \langle \boldsymbol{u}, \boldsymbol{F} \rangle \ , \tag{17.85}$$

which correctly identifies $\boldsymbol{\sigma} \cdot \hat{\boldsymbol{n}} = -\boldsymbol{F}/4\pi a^2$ as the surface tractions on a sphere translating while exerting a force $\boldsymbol{F}$ on the fluid. Again, to repeat the main theme: The Riesz theorem guarantees both the existence and uniqueness of the RBM surface tractions in this role.

We are now ready to consider the iterative solution of the tractions in a mobility problem. Consider again N particle surfaces S_i surrounded by a container surface S_c, the interior fluid domain being bound between these. As in the previous section $\boldsymbol{\varphi}_{ij}$ denote the orthonormalized particle RBMs, explicitly given by

$$\boldsymbol{\varphi}_{ij}(\boldsymbol{\xi}) = \boldsymbol{U}_{ij} + \boldsymbol{\omega}_{ij} \times (\boldsymbol{r} - \boldsymbol{r}_i) \tag{17.86}$$

on S_i and vanishing elsewhere. It is natural to choose $\boldsymbol{r}_i$ as the center of mass of the surface S_i, as has been discussed previously. The adjoint eigenfunction $\boldsymbol{\psi}_t$ is also defined as in the previous section. Given $\boldsymbol{u}$ we can solve the equation $(1 + \mathcal{H})\boldsymbol{\varphi} = \boldsymbol{u}$ and the resulting RBM components ("absorbing" the total forces and torques not representable by the double layer) are given by $-\boldsymbol{\varphi}_{ij}\langle \boldsymbol{\varphi}, \boldsymbol{\varphi}_{ij} \rangle$, as is seen by expanding $\mathcal{H}$:

$$\boldsymbol{\varphi}_{ij}\langle \boldsymbol{\varphi}, \boldsymbol{\varphi}_{ij} \rangle = -(1 + \mathcal{K})\boldsymbol{\varphi} + (\boldsymbol{u} - \boldsymbol{\psi}_t \langle \boldsymbol{\varphi}, \boldsymbol{\psi}_t \rangle) \ . \tag{17.87}$$

The effect of the ψ_t-term is to correct $\boldsymbol{u}$ to mass conserving in case it was not that to start with. The resulting RBM is thus completely characterized by the inner products on the LHS here. Consider one such inner product. The mapping $\boldsymbol{u} \mapsto \langle \varphi, \varphi_{ij} \rangle$ is a linear functional, and thus by the Riesz representation theorem this image is of the form $\langle \boldsymbol{u}, \boldsymbol{w} \rangle$ for some fixed $\boldsymbol{w}$.

Now fixing $\boldsymbol{w}$, we may insert various $\boldsymbol{u}$ in Equation 17.87 and inspect the result, $\langle \boldsymbol{u}, \boldsymbol{w} \rangle$, to identify $\boldsymbol{w}$. If $\boldsymbol{u} \in R(1+\mathcal{K})$, the inner products must all vanish in Equation 17.87. Thus $\boldsymbol{w} \perp R(1+\mathcal{K})$, or $\boldsymbol{w} \in N(1+\mathcal{K}^*)$. The latter shows that $\boldsymbol{w} = \hat{\boldsymbol{n}} \cdot \boldsymbol{\sigma}(; \boldsymbol{v})$ for some RBM $\boldsymbol{v}$, according to Theorem 3. Similarly testing with $\boldsymbol{u} = \boldsymbol{\psi}_t$ shows that $\boldsymbol{w} \perp \boldsymbol{u} = \boldsymbol{\psi}_t$, which, in physical terms, removes the pressure indeterminacy in the tractions within a bounded fluid domain. An easy way to show the last result is to note that the solution for φ is the container null function $\boldsymbol{\psi}_t \in N(1+\mathcal{K})$, so that $\langle \boldsymbol{u}, \boldsymbol{w} \rangle = \langle \varphi, \varphi_{ij} \rangle = \langle \boldsymbol{\psi}_t, \varphi_{ij} \rangle = 0$.

Let $\boldsymbol{w} \perp \boldsymbol{\psi}_t$ (and also $\boldsymbol{w} \perp R(1+\mathcal{K})$) be the tractions of some RBM $\boldsymbol{v}$. Applying $\langle \cdot, \boldsymbol{w} \rangle$ to Equation 17.87 above now gives

$$\begin{aligned} \langle \boldsymbol{u}, \boldsymbol{w} \rangle &= \langle \varphi, \varphi_{ij} \rangle \langle \varphi_{ij}, \boldsymbol{w} \rangle \\ &= \langle \varphi, \varphi_{ij} \rangle \langle \varphi_{ij}, \hat{\boldsymbol{n}} \cdot \boldsymbol{\sigma}(; \boldsymbol{v}) \rangle \\ &= -\langle \varphi, \varphi_{ij} \rangle (\boldsymbol{F}_i \cdot \boldsymbol{U}_{ij} + \boldsymbol{T}_i \cdot \boldsymbol{\omega}_{ij}) \,, \end{aligned} \tag{17.88}$$

where $\boldsymbol{F}_i$ *and* $\boldsymbol{T}_i$ *are the external total forces and torques affecting the particles relative to the points* $\boldsymbol{r}_i$ *(exerted by the particles on the fluid), corresponding to the mobility solution* $\boldsymbol{v}$. This discussion provided us another view to the significance of the "mobility-based" RBM-tractions, *avoiding the use of the Lorentz theorem and illustrating the functional analysis viewpoint.*

Now we look at things in the reversed way. Given a mobility problem for which we want to calculate the resulting RBM tractions, we start by defining

$$\varphi_g = -\varphi_{ij} (\boldsymbol{F}_i \cdot \boldsymbol{U}_{ij} + \boldsymbol{T}_i \cdot \boldsymbol{\omega}_{ij}) \,, \tag{17.89}$$

inspired by the RHS of the previous equation. Now for *any* φ

$$\langle \varphi, (1+\mathcal{H}^*) \boldsymbol{w} \rangle = \langle (1+\mathcal{H}) \varphi, \boldsymbol{w} \rangle = \langle \boldsymbol{u}, \boldsymbol{w} \rangle = \langle \varphi, \varphi_g \rangle \,, \tag{17.90}$$

and $\boldsymbol{w} = \hat{\boldsymbol{n}} \cdot \boldsymbol{\sigma}(; \boldsymbol{v})$ can be solved from

$$(1+\mathcal{H}^*) \boldsymbol{w} = \varphi_g \,. \tag{17.91}$$

The (real) spectrum of $\mathcal{H}^*$ coincides with that of $\mathcal{H}$, and iterative solution is similarly possible. In fact

$$(1 - \mathcal{P}_R/2)(1+\mathcal{H}^*)(1 - \mathcal{P}_L/2) = 1 + \tilde{\mathcal{H}}^* \,, \tag{17.92}$$

and the sequential steps of the solution are

$$\tilde{\varphi} = (1 - \mathcal{P}_R/2) \varphi_g \tag{17.93}$$

$$(1 + \tilde{\mathcal{H}}^*) \tilde{\boldsymbol{w}} = \tilde{\varphi} \tag{17.94}$$

$$\boldsymbol{w} = (1 - \mathcal{P}_L/2) \tilde{\boldsymbol{w}} \,. \tag{17.95}$$

Thus we are now able to find the RBM tractions corresponding to a given mobility problem with just one iterative solution of a linear system. Moreover, the linear system is just the adjoint of that used for solving the RBM velocities, meaning in practice that the transposed real discrete system is used. Thus some savings are possible by solving "simultaneously" these two sets of quantities, velocities, and tractions, as the elements of the system matrices are the same and need to be generated but once.

We conclude this subsection with an illustration of how these ideas apply to a single sphere. Our illustration for the sphere, which we chose for pedagogical reasons (an analytic solution is feasible), should not obscure the fact that the iterative approach is most attractive for *numerical solution* of more complex geometries.

For the RBM translation of a single, torque-free sphere in unbounded flow, we set $\mathcal{P}_R = \mathbf{0}$ (no container), and drop the particle index i above. The sequential steps of the solution simplify to

$$\begin{aligned} \tilde{\varphi} &= \varphi_g = -\boldsymbol{U}_j(\boldsymbol{F}\cdot\boldsymbol{U}_j) && (17.96)\\ (1+\tilde{\mathcal{H}}^*)\tilde{w} &= \tilde{\varphi} && (17.97)\\ w &= (1-\mathcal{P}_L/2)\tilde{w}\ . && (17.98) \end{aligned}$$

The orthonormalized translational velocities $\boldsymbol{U}_j$ will eventually be replaced with $\boldsymbol{U}_j = \boldsymbol{e}_j/|S|^{1/2}$.

For the single sphere, we fortunately know the eigensystem completely and may spectrally decompose the double layer operator as

$$1+\mathcal{K} = 1+\sum_k \lambda_k \mathcal{P}_k\ . \tag{17.99}$$

Here, $\{\mathcal{P}_k\}$ is an orthogonal family of self-adjoint projections onto the eigenspace N_{λ_k}. The physical deflation simply removes N_{-1}, so that

$$1+\mathcal{H} = 1+\sum \lambda_k \mathcal{P}_k\ ,\quad \lambda_k \in (-1,1]\ . \tag{17.100}$$

The mathematical deflation at the other end of the spectrum is accomplished with $\mathcal{P}_L = \hat{\boldsymbol{n}}\langle\cdot,\hat{\boldsymbol{n}}\rangle/|S|$, and

$$\begin{aligned} (1-\frac{1}{2}\mathcal{P}_L)(1+\mathcal{H}) &= (1+\tilde{\mathcal{H}})\\ &= 1+\sum \lambda_k \mathcal{P}_k\ ,\quad \lambda_k \in (-1,1)\ . \end{aligned}$$

Since the projection operators in question are self-adjoint, so is $\mathcal{H}$ and the decomposition

$$(1+\tilde{\mathcal{H}}^*) = 1+\sum \lambda_k \mathcal{P}_k\ ,\quad \lambda_k \in (-1,1) \tag{17.101}$$

is obtained. The iterative procedure reduces to

$$\tilde{w} = -\left(\sum_k \lambda_k \mathcal{P}_k\right)\tilde{w} - \boldsymbol{U}_j(\boldsymbol{F}\cdot\boldsymbol{U}_j)\ ,\quad \lambda_k \in (-1,1)\ , \tag{17.102}$$

with the solution, $\tilde{\boldsymbol{w}} = -\boldsymbol{U}_j(\boldsymbol{F}\cdot\boldsymbol{U}_j)$, obtained immediately after just the first iteration from the fact that $\boldsymbol{U}_j \in N_{-1} \perp N_{\lambda_k}$.

Finally, the RBM traction, $\boldsymbol{w} = \boldsymbol{\sigma}\cdot\hat{\boldsymbol{n}}$, is obtained as follows:

$$\begin{aligned}\boldsymbol{w} &= (1-\frac{1}{2}\mathcal{P}_L)\tilde{\boldsymbol{w}} = -(1-\frac{1}{2}\mathcal{P}_L)\boldsymbol{U}_j(\boldsymbol{F}\cdot\boldsymbol{U}_j)\\ &= -\boldsymbol{U}_j(\boldsymbol{F}\cdot\boldsymbol{U}_j) = -\frac{1}{4\pi a^2}\boldsymbol{e}_j(\boldsymbol{F}\cdot\boldsymbol{e}_j) = -\frac{\boldsymbol{F}}{4\pi a^2},\end{aligned}$$

and this is indeed the correct result.

Exercises

Exercise 17.1 The Double Layer Kernel on a Sphere.
Show that $\mathcal{K}$ is self-adjoint on a single sphere. How does this imply the result of Exercise 15.4?

Exercise 17.2 Complex Stokes Solutions.
Verify the complex form of the Lorentz reciprocal theorem, given when discussing the spectrum of the double layer operator.
Hint: Note that while $\langle \imath a, b\rangle = \imath\langle a, b\rangle$, the conjugate linearity with respect to the second argument implies that $\langle a, \imath b\rangle = -\imath\langle a, b\rangle$.

Exercise 17.3 Ill-Posedness of the First-Kind Equation.
In Chapter 1, we gave a heuristic argument, using highly oscillatory inputs, on why integral equations of the first kind were ill-posed problems. However, since the Oseen tensor $\mathcal{G}(\boldsymbol{x})$ is singular at the origin, we may ask whether this singular behavior somehow saves us, *i.e.*, the well-conditioned property of the second-kind equation is mimicked to some extent. The answer, of course, is no, as this exercise with a sphere shall illustrate.

Consider high-frequency velocity fields of the form $\nabla\Phi_{-n-1}$, the exterior vector harmonic in Lamb's general solution. Consider the integral representation for this velocity field in the region outside a unit sphere, use the fact that the tractions on the sphere surface are given by $-2(n+2)\mu\nabla\Phi_{-n-1}$, and that $\nabla\Phi_{-n-1}|_{r=1}$ is an eigenfunction of the double layer operator to derive the following relation:

$$\frac{1}{2}\nabla\Phi_{-n-1} = \frac{(n+2)}{4\pi}\oint \nabla\Phi_{-n-1}\cdot\mathcal{G}\,dS + \frac{1}{2}\lambda_n^+\nabla\Phi_{-n-1}$$

or

$$\oint \nabla\Phi_{-n-1}\cdot\mathcal{G}dS = \frac{8\pi n\nabla\Phi_{-n-1}}{(2n+1)(2n+3)}.$$

This shows that for large n, the output becomes small. This also explains why in practice we may use the single layer representation for spheres and other smooth particles of moderate aspect ratios, since the higher oscillations are suppressed by the use of coarse meshes. For oblate spheroids, we find that the

behavior is essentially the same, until the aspect ratio approaches 10; then the large tractions near the rim imply that the factor of n gets amplified. Thus the ill-conditioning is a significant problem, especially when fine meshes are used at the rim.

Exercise 17.4 The Spectral Radius of the Single Layer Operator.
Consider the single layer operator mapping ψ to

$$\frac{1}{4\pi\mu}\oint_S \mathcal{G}\cdot\psi\, dS\ .$$

Consider the effect of rescaling a particle surface, say by factor a. Find the power of a by which the spectrum of the single layer operator gets scaled. Plot some of the eigenvalues implicitly given for a unit sphere in Exercise 17.3.
Note: This is the reason why no bounds can be given, without some restrictions to particle size, for the spectral radius of the single layer operator.

Exercise 17.5 Diagonalizability of a Square Matrix.
Show that a square matrix can be diagonalized if and only if it can be expressed as the product of a symmetric positive definite (SPD) and a symmetric matrix.
Solution: Assume diagonalizability, $A = P^{-1}DP$. Then also

$$A = (P^{-1}P^{-T})(P^TDP)\ ,$$

where we have an SPD matrix multiplying a symmetric one. Assume $A = BC$, where B is SPD and C symmetric. Then $A = B^{1/2}(B^{1/2}CB^{1/2})B^{-1/2}$, and diagonalizing the symmetric matrix in the parentheses to $Q^{-1}DQ$ gives the diagonal representation of A with $P = QB^{-1/2}$.
Note: According to the Lorentz reciprocal theorem the mapping of velocity BCs to corresponding tractions is symmetric (just write the theorem in inner product notation), and it is also positive *semi*definite due to the energy relation. Thus the operator product is almost of the form given in the exercise above, when this operator is applied after the symmetric mapping of a single layer density to corresponding surface velocity. (The symmetry of this mapping is visible from the symmetric kernel, namely, the Green's function.) From this we may conjecture that the operator $\mathcal{K}^*$ should be diagonalizable, the same equivalently holding for $\mathcal{K}$. In fact Odqvist has shown that the Jordan blocks for $|\lambda| \neq 1$ are trivial, and this (together with our theorems regarding the extreme eigenvalues) implies the diagonalizability of $\mathcal{K}$. Therefore the discussion of nontrivial Jordan blocks in connection with Wielandt's deflation was somewhat superfluous for our application and only served the purpose of generality.

Exercise 17.6 Tractions via the Reciprocal Theorem: Rate-of-Strain Fields.
Let $\boldsymbol{E}$ be a symmetric traceless 3×3 matrix, generating the Stokes velocity field $\boldsymbol{v} = \boldsymbol{E}\cdot\boldsymbol{x}$. For convenience assume that the viscosity $\mu = 1$. First recall that the rate-of-strain tensor and the stress tensor of this field both coincide

with $\boldsymbol{E}$. Derive a system of well-posed equations from which the tractions of the disturbance field cancelling $\boldsymbol{v}$ on a particle surface could be solved numerically. **Solution:** Denote the disturbance field by $\boldsymbol{v}_d$ and its traction surface field by $\boldsymbol{w} = \hat{\boldsymbol{n}} \cdot \boldsymbol{\sigma}(;\boldsymbol{v}_d)$. An arbitrary disturbance field can be represented on S by $\boldsymbol{u} = (1+\mathcal{K})\boldsymbol{\varphi} + (\boldsymbol{F} - \frac{1}{2}\boldsymbol{T} \times \nabla) \cdot \mathcal{G}/(8\pi\mu)$. Applying Lorentz reciprocal theorem to the double layer part of $\boldsymbol{u}$, one finds $\langle (1+\mathcal{K})\boldsymbol{\varphi}, \boldsymbol{w}\rangle = \langle \hat{\boldsymbol{n}} \cdot \boldsymbol{\sigma}(;\mathcal{K}\boldsymbol{\varphi}), \boldsymbol{v}_d\rangle = \langle \hat{\boldsymbol{n}} \cdot \boldsymbol{\sigma}(;\mathcal{K}\boldsymbol{\varphi}), -\boldsymbol{v}\rangle = \langle (-1+\mathcal{K})\boldsymbol{\varphi}, \hat{\boldsymbol{n}} \cdot \boldsymbol{\sigma}(;-\boldsymbol{v})\rangle = -\langle (-1+\mathcal{K})\boldsymbol{\varphi}, \hat{\boldsymbol{n}} \cdot \boldsymbol{E}\rangle$, where the second application of the Lorentz reciprocal theorem was on the double layer generated velocity field and $\boldsymbol{v}$ *inside* the particle. Since $\boldsymbol{\varphi}$ is arbitrary, this gives the equation $(1+\mathcal{K}^*)\boldsymbol{w} = -(-1+\mathcal{K}^*)(\hat{\boldsymbol{n}} \cdot \boldsymbol{E})$. The operator acting on $\boldsymbol{w}$ is not invertible, and bordering will have to be used here. The added equations come from the force and torque terms: $\langle \hat{\boldsymbol{e}}_i \cdot \mathcal{G}, \boldsymbol{w}\rangle = \langle \hat{\boldsymbol{n}} \cdot \boldsymbol{\sigma}(;\hat{\boldsymbol{e}}_i \cdot \mathcal{G}), -\boldsymbol{v}\rangle$ and $\langle (\hat{\boldsymbol{e}}_i \times \nabla) \cdot \mathcal{G}, \boldsymbol{w}\rangle = \langle \hat{\boldsymbol{n}} \cdot \boldsymbol{\sigma}(;(\hat{\boldsymbol{e}}_i \times \nabla) \cdot \mathcal{G}), -\boldsymbol{v}\rangle$, for $i \in \{1,2,3\}$. Since the range of $(1+\mathcal{K}^*)$ is orthogonal to RBM velocities, the six added variables can be defined as components of translation and rotation velocities, modifying the equation to $(1+\mathcal{K}^*)\boldsymbol{w} + \boldsymbol{U} + \boldsymbol{\omega} \times \boldsymbol{\xi} = -(-1+\mathcal{K}^*)(\hat{\boldsymbol{n}} \cdot \boldsymbol{E})$. In fact, the added variables should get value zero, but in a numerical approximation this will not be exactly so.

Exercise 17.7 Deflations Over Bordering.
From your favorite text on numerical methods, check the number of operations required for the solution of a linear system of dimension m by Gaussian elimination. It should be $O(m^3)$. Consider now the iterative solution of a system of the same size. Convince yourself that each iterative step takes $O(m^2)$ operations. Since the rate of convergence depends on the largest eigenvalue, close to that of the continuous system approximated, it will stay about the same as the discretization is refined. Therefore the iterative solution with different discretizations but the same initial guess will take also $O(m^2)$ operations. This shows a definite advantage for the iterative solution when accurate results are desired.

Consider now a single particle, the deflated system size being m and the bordered system size $m+6$. For solving a *resistance problem* you have the following choices:

1. Solve iteratively six mobility problems and construct the mobility matrix, then solve by elimination one problem with the mobility matrix as the system matrix.
2. Solve directly by elimination the bordered system.

Which one is more advantageous? Show that if the iterative solutions above are changed to elimination solutions, the bordering scheme becomes more efficient for large m.

Exercise 17.8 Double Layer Eigenfunctions for the Ellipsoid.
In this chapter, we saw that the double layer density in the solution for a sphere in the constant rate-of-strain field $\boldsymbol{E} \cdot \boldsymbol{x}$ is an eigenfunction of $\mathcal{K}$, with eigenvalue $-1/5$. Show that the solutions for a torque-free ellipsoid in the constant rate-of-strain field are eigenfunctions of $\mathcal{K}$, and determine the expression for the

eigenvalues in terms of elliptic integrals. Look at the degenerate case of ellipsoids of revolution and examine what happens to the various families of eigenfunctions with increasing nonsphericity. Do your results suggest that numerical difficulties will be encountered in the numerical solution for flow past nearly flat oblate spheroids and very slender prolate spheroids?

Exercise 17.9 Perturbation Results for the Two-Sphere Spectrum. In this chapter, we computed the spectral radius of the two-sphere system, at large R, by a perturbation solution on the single-sphere eigenvalue $\lambda = -3/5$. Generalize this approach to determine the splitting induced by hydrodynamic interactions on the entire spectrum of the single sphere. Do the eigenvalues cross as R is reduced?

Exercise 17.10 Double Layer Representation for Axisymmetric Flow. For axisymmetric problems (symmetry axis $\boldsymbol{d} = -\boldsymbol{e}_z$), show that a velocity field $\boldsymbol{v}$ with the multipole representation

$$\boldsymbol{v} = \sum_{n=0}^{\infty} \left\{ A_n \frac{(\boldsymbol{d}\cdot\nabla)^n}{n!}\boldsymbol{d}\cdot\mathcal{G} + B_n \frac{(\boldsymbol{d}\cdot\nabla)^n}{n!}\boldsymbol{d}\cdot\nabla^2\mathcal{G} \right\}$$

may also be written in terms of a double layer density on a unit sphere,

$$\boldsymbol{v}(\boldsymbol{x}) = A_0\boldsymbol{d}\cdot\mathcal{G}(\boldsymbol{x}) + \oint_S \boldsymbol{K}(\boldsymbol{x},\boldsymbol{\xi})\cdot\boldsymbol{\varphi}\, dS \ ,$$

with the double layer density given by

$$\boldsymbol{\varphi}(\boldsymbol{\xi}) = \sum_{n=1}^{\infty} \alpha_n \boldsymbol{\varphi}^-_{n+1}(\boldsymbol{\xi}) + \sum_{n=0}^{\infty} \beta_n \boldsymbol{\varphi}^+_{n+1}(\boldsymbol{\xi}) \ .$$

This result is used in the subsequent problems.

Exercise 17.11 Use of an Off-Center Stokeslet in Range Completion. Use the results of the previous exercise to derive the double layer density for a sphere of radius a translating with velocity $\boldsymbol{U}$ with an off-center Stokeslet completing the representation. Assume that the Stokeslet and the the displacement R are all in the direction of $\boldsymbol{U}$. The final result may be written as

$$\begin{aligned}
\boldsymbol{\varphi}(\boldsymbol{\xi}) &= -\frac{5\boldsymbol{F}}{48\pi\mu a}\cdot(\hat{\boldsymbol{n}}\hat{\boldsymbol{n}} - \frac{1}{3}\boldsymbol{\delta}) \\
&+ \frac{F}{8\pi\mu a}\sum_{n=2}^{\infty}\left\{ \frac{(R/a)^{n-1}}{2(n-1)}\left[\boldsymbol{e}_r n P_n(\cos\theta) + \boldsymbol{e}_\theta \frac{\partial P_n}{\partial\theta}\right]\right. \\
&\quad + \left(\frac{(R/a)^{n-1}}{2n+1} - \frac{(R/a)^{n+1}}{2n+3}\right)\frac{n(2n+1)(2n+3)}{2(2n^2+4n+3)} \\
&\quad \left.\times\left[-\boldsymbol{e}_r(n+1)P_n(\cos\theta) + \boldsymbol{e}_\theta\frac{\partial P_n}{\partial\theta}\right]\right\} \ .
\end{aligned}$$

Note that with increasing eccentricity, the double layer density becomes highly oscillatory. This is a typical symptom of a poor choice for the range completion.

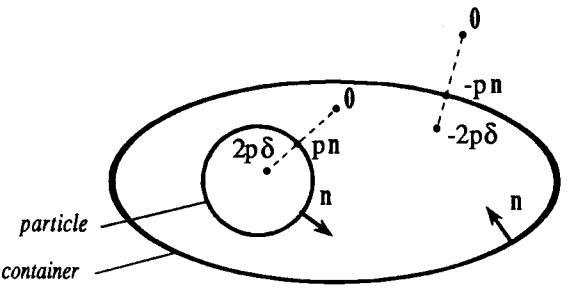

Figure 17.5: Geometry for the single layer eigenfunction with zero dissipation; stress fields of the single layer potential of density $p\hat{n}$ (on a particle surface and on a container surface).

Exercise 17.12 Oseen's Image for a Stokeslet Near a Sphere.
In Part III, we derived a multipole representation for the Oseen image for a Stokeslet near a rigid sphere. Use the result of Exercise 17.10 to express the image of an Stokeslet directed along the axis as a completed double layer representation. In this case, what is the best way of completing the range if a single Stokeslet is used? What is the best way of completing the range if a line distribution of Stokeslets is employed?

Exercise 17.13 Single Layer Eigenfunctions with Zero Total Dissipations.
Let ψ be a single layer eigenfunction (corresponding to an eigenvalue λ) on the totality of bounding surfaces S, and suppose that the velocity fields induced by ψ have zero total dissipation (sum of dissipations in the interior and the exterior domains). As discussed in Section 17.2, the condition of zero dissipation forces the single layer density to be a multiple of the surface normal on each surface, *viz.*, $p\hat{n}$. Since the traction *drops* by $2p$ across the surface and since the stresses must be zero on the "outsides" we obtain the situation shown in Figure 17.5 for the surface values of the single layer potential. Now on each surface apply the condition that ψ is an eigenfunction. Show that this forces the eigenvalue λ to be either -1 or $+1$.